



Effect of uncertainties of Southern Ocean surface temperature and sea-ice change on Antarctic climate projections

Julien Beaumet¹, Michel Déqué², Gerhard Krinner¹, Cécile Agosta^{3,4,1}, and Antoinette Alias²

¹Univ. Grenoble Alpes, CNRS, Institut des Géosciences de l'Environnement, F-38000, Grenoble, France

²CNRM, Université de Toulouse, Météo-France, CNRS, Toulouse, France

³F.R.S.-FNRS, Laboratory of Climatology, Department of Geography, University of Liège, B-4000 Liège, Belgium

⁴Laboratoire des Sciences du Climat et de l'Environnement (IPSL/CEA-CNRS-UVSQ UMR 8216), CEA Saclay, F-91190 Gif-sur-Yvette, France

Correspondence to: Julien Beaumet (Julien.Beaumet@univ-grenoble-alpes.fr)

Abstract. In this study, the atmospheric model ARPEGE is used with a stretched grid in order to reach a average horizontal resolution of 35 kilometers over Antarctica. Over the historical period (1981-2010), ARPEGE is forced by the historical sea surface conditions (SSC, i.e. sea surface temperature and sea-ice concentration) from MIROC and NorESM1-M CMIP5 historical runs and by observed SSC (AMIP-experiment). These three simulations are evaluated against ERA-Interim for atmospheric general circulation and against MAR regional climate model and *in-situ* observations for surface climate. As lower boundary conditions for simulations for the period 2071-2100, we use SSC from coupled climate model CMIP5 simulations of the same models following the RCP8.5 emission scenario. We use these output both directly and with an anomaly method based on quantile mapping. We assess the uncertainties linked to the choice of the coupled model and the impact of the method (direct output and anomalies). For the simulation using SSC from NorESM1-M, we do not find significant changes in climate change signals over Antarctica when using bias-corrected SSC. For the simulation using MIROC-ESM output, an additional increase of +185 Gt yr⁻¹ in precipitation and of +0.8 K in winter temperatures for the grounded Antarctic ice-sheet was obtained when using bias-corrected SSC.

Copyright statement.

1 Introduction

15 Dominated by precipitation increase, the surface mass balance (SMB) of the Antarctic ice sheet is the only projected negative contributor to the global eustatic sea level rise (SLR) over the course of the 21st century (Agosta et al., 2013; Ligtenberg et al., 2013; Lenaerts et al., 2016; Palermé et al., 2017). However, the acceleration of ice dynamics and the interactions between oceans and ice-shelves are expected to yield an overall positive Antarctic contribution to SLR (Pollard et al., 2015; Ritz et al., 2015). For these reasons, it is crucial to produce downscaled Antarctic climate scenarios for the end of the current century with
20 reduced uncertainties in order to provide i) better estimates of the contribution of the ice-sheet SMB and ii) better accumulation



or atmospheric forcings for ice dynamics and ocean-ice-shelfs interactions studies.

The attribution of recent evolutions of the Antarctic climate to the current anthropic climate change is more challenging compared to the Arctic. Indeed, while some parts of West Antarctica and of the Antarctic Peninsula have experienced one of the world's most dramatic warming in the second part of the 20th century (Vaughan et al., 2003; Bromwich et al., 2013), there was
5 no significant trend in the evolution of the temperatures of East Antarctica as a whole (Nicolas and Bromwich, 2014) except for some coastal regions that experienced a cooling in autumn over the 1979-2014 period (Clem et al., 2018). Moreover, the observed strong warming trend in the Antarctic Peninsula has shown a pause or even a reversal for 13 years in the beginning of the 21st century (Turner et al., 2016). Contrary to the dramatic sea ice loss observed in the Arctic (e.g., Stroeve et al., 2012), significant positive trends have been observed in the sea-ice around Antarctica since the 1970s (Comiso and Nishio,
10 2008; Turner et al., 2015, e.g.), although record sea ice loss was observed in 2016/7 (Turner et al., 2017). Most of the Coupled Atmosphere-Ocean Global Circulation Models (AOGCM or CGCM) such as those participating the Coupled Model Intercomparison Project, Phase 5 (CMIP5, Taylor et al. (2012)) struggle to reproduce the seasonal cycle of Sea-Ice Extent (SIE) around Antarctica, and very few of them was able to reproduce the positive trend observed in the end of the 20th century (Turner et al., 2013). This is a major issue as the evolution of the Antarctic climate by the end of the current century was shown to be more
15 sensitive to the evolution of the sea surface conditions (SSC), i.e. sea surface temperatures (SST) and sea-ice concentration (SIC), than to the evolution of greenhouse gases concentration (Krinner et al., 2014). Besides, the amount of sea-ice present in the historical AOGCM climate simulation is strongly correlated to the absolute decrease in sea-ice in the projections for the 21st century (Agosta et al., 2015), which is itself strongly linked to the strengthening of the westerly winds maximum (Bracegirdle et al., 2018).
20 So far, it is expected that the signal due to the current anthropic climate change will take over the natural variability of Antarctic climate by the middle of the twenty-first century (Previdi and Polvani, 2016). A more complete review of the current understanding of the regional climate and surface mass balance of Antarctica and of the key-processes that need to be taken into account in order to assess their evolution can be found in Favier et al. (2017).

25 The dynamical downscaling of climate scenarios such as those provided by coupled models from the CMIP5 experiment is generally performed using regional climate models (RCM). The marginal importance of atmospheric deep convection for Antarctic precipitations does not require to perform dynamical downscaling at very high resolutions allowing the use of a cloud resolving atmospheric model configuration. The added value of simulations at a higher resolution, for instance CORDEX-like simulations (Giorgi and Gutowski, 2016) at 0.44°, with respect to original climate scenario at a coarser resolution (1 to 2°) is
30 significant in coastal regions near the ice-sheet margins or on the Antarctic Peninsula, as the steep topography induces a strong precipitation gradient between wet coastal regions and dry inland Antarctic Plateau. Below 1000 m above sea level (a.s.l), the origin of precipitations on the Antarctic continent is mostly orographic (e.g., Orr et al., 2008). As a consequence, model ran at a higher horizontal resolution tend to produce higher estimates of the snow accumulation at the continent scale over Antarctica and higher accumulation increases in a warming climate (Genthon et al., 2009; Agosta et al., 2013). Modelling of strong



katabatic winds that blow at the ice sheet surface is also generally improved with a better representation of the topography (e.g., van Lipzig et al., 2004).

In this study, we use CRNM-ARPEGE, the atmosphere general circulation model (AGCM) from Météo-France, with a stretched grid allowing a horizontal resolution of about 40 km over the whole Antarctic continent, to dynamically downscale
5 different climate scenarios. As a global atmospheric model, ARPEGE is driven by prescribed SSC, but does not require any lateral boundary conditions. More details on the model setup are given in section 2.1. This method has some advantages over the more commonly use of RCM. It is possible to use observed SSC at the present and model-generated SSC anomalies for projections (e.g., Krinner et al., 2008). When such an anomaly method is used, the results do not absolutely require the AOGCM used as driver for sea surface conditions to represent the atmospheric general circulation and its variability in the
10 region of interest realistically in every respect. Using a stretched grid GCM also allows better taking into account potential feedbacks and teleconnections between the high-resolution region which the focus lies on, and other regions of the world. Rather unsurprisingly, several studies showed that AGCMs produce a better representation of atmospheric general circulation and a better repartition of precipitation when forced by observed instead of simulated SSC (Krinner et al., 2008; Ashfaq et al., 2011; Hernández-Díaz et al., 2017). These studies also showed that bias correction of SSC before the downscaling of future
15 climate scenarios gives significantly different results with respect to original scenarios. For these reasons, we performed a bias-correction of SSC using a quantile mapping method for SST and an analog method for SIC following the methods and recommendations described in Beaumet et al. (2018).

We reduced our ensemble of possible simulations to the choice of two AOGCMs from the CMIP5 experiment : MIROC-ESM and NorESM1-M. As they are bias-corrected in a second step, the main criterion was the amplitude of the climate change signal
20 in the oceanic forcings coming from these two models, not the realism of the simulated present-day SSC. The short analysis on which we based our model choice is described in section 2.2. We also performed an AMIP-style control simulation for the period 1981-2010 in which CNRM-ARPEGE is forced by observed SST and SIC coming from PCMDI data set (Taylor et al., 2000). CNRM-ARPEGE was also forced by the original oceanic SSC coming from the historical simulations of MIROC-ESM and NorESM1-M (1981-2010) and from projections under the radiative concentration pathway RCP8.5 (Moss et al., 2010)
25 carried out with the same two models (2071-2100). In section 3.1, we present the ability and limitations of CNRM-ARPEGE to represent current Antarctic climate as well as the differences between the AMIP experiment and the experiments forced by oceanic forcings coming from historical simulations of CMIP5 GCMs. In section 3.2, we present modelled climate at the end of the 21st century by CNRM-ARPEGE and the differences in climate change signal between scenarios realized with bias-corrected and original SSC from the RCP8.5 scenarios of MIROC-ESM and NorESM1-M.

30 2 Data and Methods

2.1 Sea Surface Conditions in CMIP5 AOGCMs

SSC forcings have been identified as key forcings for the evolution of the Antarctic climate of the continent (Krinner et al., 2014; Agosta et al., 2015). In this study, SSC obtained from CMIP5 projections are bias-corrected using recommendations and



methods from Beaumet et al. (2018) before being used as surface boundary conditions for the atmospheric model. Therefore, the importance of the bias of each CMIP5 model for the reconstruction of oceanic conditions around Antarctica in their historical simulation is reduced. There is however a limitation in the previous statement, as the analog method used to bias-correct SIC runs into trouble when the bias is so large that sea ice completely disappears over wide areas for too long. Besides this
5 caveat, however, the choice of CMIP5 AOGCMs used in this study was guided by compliance to desired characteristics of the climate change signal rather than by the skills of the models in reproducing SSC in the historical periods.

Therefore, we identified CMIP5 models with the highest and lowest climate change signal by the end of the 21st century considering only SSC in the Southern Ocean, in order to span the uncertainty range associated with model response. We computed the relative evolution of integrated winter SIE over the whole Southern Ocean between the historical simulation (reference
10 period: 1971-2000) and the RCP8.5 scenario (reference period: 2071-2100) for 21 AOGCMs from CMIP5 experiment. The CMIP5 ensemble was reduced to 21 because some models sharing the same history of development and high code comparability as others have been discarded. The model list is the same as in Krinner and Flanner (2017) and can be seen in the Fig. 1 legend. We also looked at the mean summer SST increase South of 60°S for the same reference periods. In order to be consistent with periods of maximum (minimum) SIE, seasons considered in this analysis are slightly shifted, and winter
15 (summer) correspond here to the period August-September-October, ASO (February-March-April, FMA).

The results of the computation can be seen in Figure 1, which displays the relative decrease of SIE in winter (ASO) in the RCP8.5 scenario as a function of the value of the mean winter SIE in the historical simulation. The four models with the highest decrease in SIE are CNRM-CM5 (-62.4%), GISS-E2-H (-53.4%), inmcm4 (-47.9%) and MIROC-ESM (-45,2%). Because of the above-mentioned limitation of the bias-correction method, the first three GCMs cannot be selected due to a large
20 negative bias of winter and spring SIE. We therefore selected MIROC-ESM as representative for models projecting a large climate change signal for sea ice around Antarctica. If we consider weak climate change signals, MIROC5 shows the lowest decrease (-1,5%) followed by NorESM1-M (-13,6%). For the same reasons of limitations of the bias correction method, we dismissed MIROC5 and kept NorESM1-M as representative for a weak climate change signals in the SSC around Antarctica. The impact of primarily considering changes in winter SIE rather than in summer SST is limited as the climate change signal
25 for these two variables are strongly linked ($R^2=0.96$). For summer SSTs, MIROC-ESM shows the 6th largest increase(+1.8K) while NorESM1-M exhibits the second lowest (+0.4K).

2.2 CNRM-ARPEGE set-up

We use version 6.2.4 of AGCM ARPEGE, a spectral primitive equation model from Météo-France, CNRM (Déqué et al., 1994). The model is run at T255 truncation with a 2.5 zoom factor and a pole of stretching at 80°S and 90°E. With this setting,
30 the horizontal resolution in the Antarctic ranges from 35 km near the stretching pole on the Antarctic Plateau to 45 km at the Northern end of the Antarctic Peninsula. At the Antipodes, near the North Pole, the horizontal resolution decreases to about 200 km. In this model version, the atmosphere is discretized into 91 sigma-pressure vertical levels. The surface scheme is SURFEX-ISBA-ES (Noilhan and Mahfouf, 1996) which contains a three-layer snow scheme of intermediate complexity (Boone and Etchevers, 2001) that takes into account the evolution of the surface snow albedo, the heat transfer through the snow

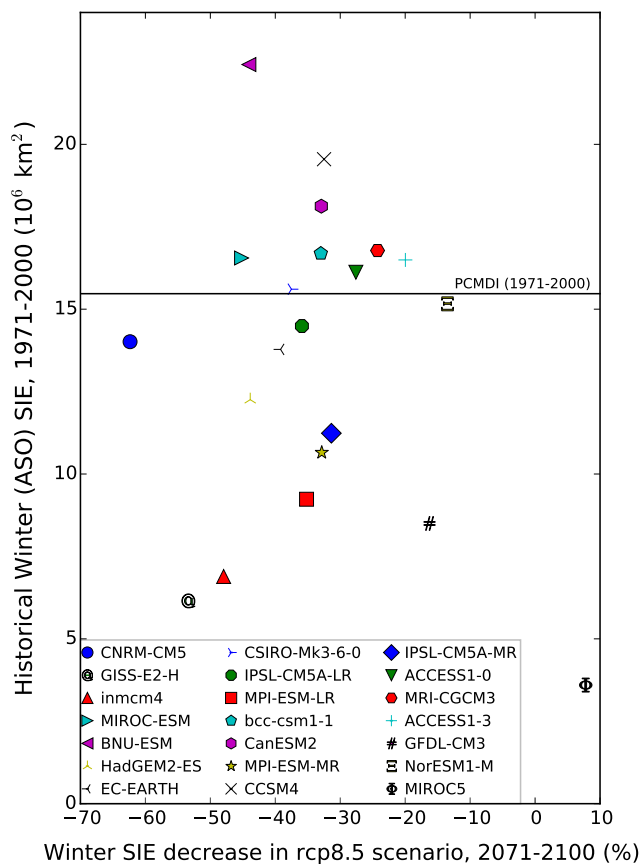


Figure 1. Historical Antarctic Winter (August-September-October: ASO) Sea-Ice Extent (SIE, in millions of km²) as function of the relative decrease of Winter SIE in the RCP8.5 scenario for the period 2071-2100 with respect to the reference period 1971-2000. The mean Winter SIE in the observations for the historical reference period is indicated by the horizontal black line (PCMDI 1971-2000).

layers and for the percolation and refreezing of liquid water in the snow pack. Over the ocean, we use a 1D version of sea-ice model GELATO (Salas y Méliá, 2002) which means that no advection of sea-ice is possible. The sea-ice thickness is prescribed following the empirical parametrization used in Krinner et al. (1997, 2010) and described in Beaumet et al. (2018). The use of GELATO is therefore limited to the computation of heat and moist fluxes in sea-ice covered regions and also allows taking

5 into account for the accumulation of snow on top of sea-ice.

In each ARPEGE simulation, the first two years are considered as a spin-up phase for the atmosphere and the soil, and are therefore discarded from the analysis. The characteristics of the different ARPEGE simulations presented in this paper are summarized in the table1.



Table 1. Summary of the period, sea surface conditions, greenhouse gases concentration and reference historical simulation for each future scenarios for each ARPEGE simulation presented in this paper

Simulations	Period	SSC	GES Concentration	Reference for hist. climate
ARP-AMIP	1981-2010	Observed	historical	-
ARP-NOR-20	1981-2010	NorESM1-M historical	historical	-
ARP-MIR-20	1981-2010	MIROC-ESM historical	historical	-
ARP-NOR-21	2071-2100	NorESM1-M RCP8.5	RCP8.5	ARP-NOR-20
ARP-MIR-21	2071-2100	MIROC-ESM RCP8.5	RCP8.5	ARP-MIR-20
ARP-NOR-21-OC	2071-2100	Bias-corrected NorESM1-M RCP8.5	RCP8.5	ARP-AMIP
ARP-MIR-21-OC	2071-2100	Bias-corrected MIROC-ESM RCP8.5	RCP8.5	ARP-AMIP

3 Results

3.1 Evaluation for Present Climate

The ability of ARPEGE model to reproduce atmospheric general circulation of the Southern Hemisphere is assessed by comparing sea level pressure (SLP) and 500 hPa geopotential (Z500) South of 20°S to those of ERA-Interim reanalysis (ERA-I). For surface climate of the Antarctic continent, several studies have shown that (near) surface temperatures from ERA-I are not reliable (Bracegirdle and Marshall, 2012; Jones and Harpham, 2013; Fréville et al., 2014), as the reanalysis is not constrained by enough observations and because the boundary layer physics of the model fails to successfully reproduce strong temperature inversions near the surface that characterize the climate of the Antarctic Plateau. As a consequence, near-surface temperatures in Antarctica from ARPEGE simulations are evaluated using observations from the SCAR READER data base (Turner et al., 2004) as well as temperatures from a MAR RCM simulation in order to increase the spatial coverage of the model evaluation. Modèle Atmosphérique Régional (MAR, Gallée and Schayes (1994)) has been one of the most successful RCMs in reproducing the surface climate of large ice-sheets such as Greenland (Fettweis et al., 2005; Lefebvre et al., 2005) and Antarctica (Gallée et al., 2015; Amory et al., 2015; Agosta et al., 2018). In this evaluation, we compare ARPEGE near surface temperatures to those of an ERA-I driven MAR simulation (hereafter MAR-ERA-I) at a similar horizontal resolution of 35 kilometres (Agosta et al., 2018). SMB of the grounded Antarctic Ice Sheet and its components from ARPEGE simulations are compared to outputs of the same ERA-Interim driven MAR simulation from Agosta et al. (2018).

3.1.1 Atmospheric General Circulation

Difference between mean SLP from the ARPEGE simulation (1981-2010) forced by observed SSC (called ARP-AMIP in the remainder of this paper, see table 1) and mean SLP from ERA-I reanalysis can be seen in Fig. 2a. The general pattern is an underestimation of SLP around 40°S, especially in the Pacific sector and an overestimation around Antarctica, especially in Amundsen/Ross sea sector. Mean SLP differences for ARPEGE simulations forced by NorESM1-M (ARP-NOR-20) and



Table 2. Seasonal root mean square error (RMSE) on mean SLP South of 20°S with respect to ERA-Interim for the different ARPEGE simulations over the 1981-2010 period.

Simulations	DJF	MAM	JJA	SON
ARP-AMIP	3.3	2.7	3.1	3.0
ARP-NOR-20	3.5	4.3	4.8	4.6
ARP-MIR-20	3.2	4.0	4.6	3.2

MIROC-ESM (ARP-MIR-20) historical SSC can be seen respectively in Fig. 2b and Fig. 2c. The pattern and the magnitude of the errors are similar to those of the ARP-AMIP simulation in summer (DJF). The root mean square errors (RMSE) per seasons for each simulations are summarized in Table 2. In winter (JJA), spring (SON) and autumn (MAM) the errors are substantially larger in ARP-NOR-20 and ARP-MIR-20 than in ARP-AMIP. The patterns of the errors and the ranking of simulations scores are similar for 500hPa geopotential height than for SLP (*not shown*).

The mean atmospheric general circulation in each simulation has also been compared and evaluated against ERA-I by analyzing the 850 hPa eastwards wind component (referred to as westerly winds in the following) latitudinal profile, as well as the strength (m/s) and position (°Southern latitude) of the zonal mean westerly wind maximum or westerly "jet" (Fig. 3). In this figure, results are only presented for the annual average, as the differences between simulations or with ERA-I do not depend much on the season considered (*not shown*). When compared with ERA-I, ARP-AMIP and ARP-MIR-20 are closer to ERA-I when the westerly winds maximum strength is considered, and ARP-NOR-20 when it is its position. With respect to ARP-AMIP, ARP-NOR-20 displays a much weaker and poleward surface westerly jet in all seasons, while ARP-MIR-20 is characterized by a lower latitude westerly wind maximum of comparable strength.

3.1.2 Near Surface Temperatures

Screen level (2m) air temperatures (T_{2m}) from ARP-AMIP simulation are compared to those of the ERA-Interim driven MAR simulation in winter (JJA) and summer (DJF) for the reference period 1981-2010. Differences are shown in Fig. 4. On the same figure, circles represent T_{2m} differences between ARP-AMIP and weather stations from the READER data base. In this analysis, weather stations where less than 80% of valid observations were recorded for the reference period were not used for the computation of climatological mean. Altitude differences between corresponding ARPEGE grid point and weather stations have been taken into account by correcting modelled temperatures with a 9.5 K km^{-1} vertical gradient. Errors on T_{2m} in ARP-AMIP simulation for each weather station and each season are presented in Tab. 3. A map showing the location of these stations can be seen in the supplementary material (Fig. B1).

The ARP-AMIP T_{2m} are warmer than MAR-ERA-I on the ridge and the western part of the Antarctic Plateau in winter as well as on the large Ronne and Ross ice-shelves. ARPEGE is colder than MAR-ERA-I on the Southern and Western part of the Antarctic Peninsula, especially in winter, which is consistent with atmospheric circulation errors. Finally, we can also mention a moderate (1 to 3K) but widespread warm bias on the slope of the East Antarctic Plateau and on the West side of the

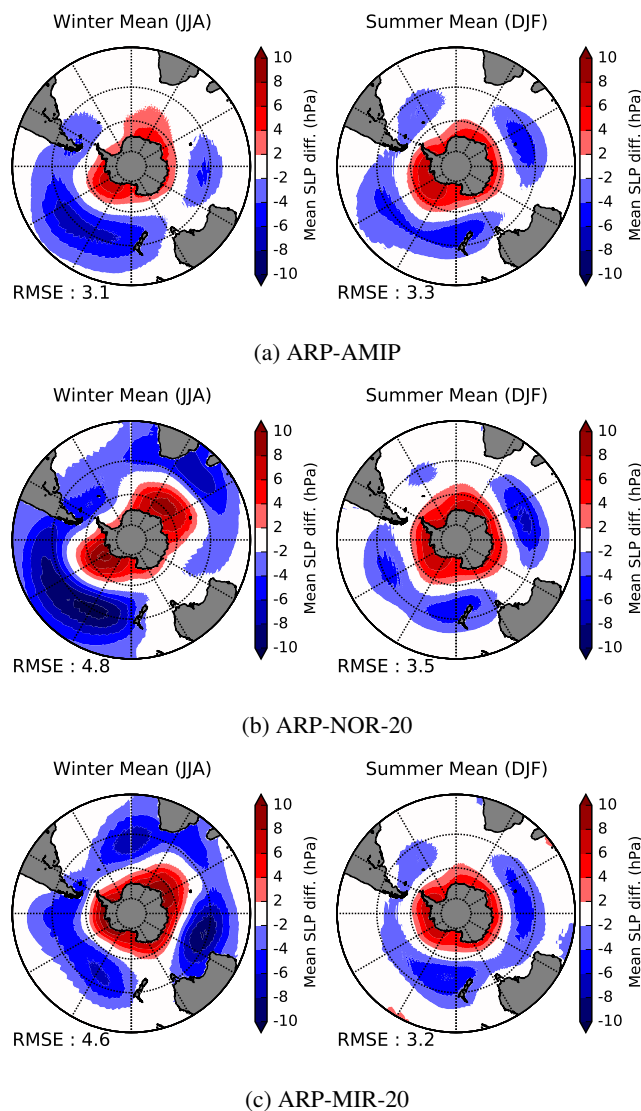


Figure 2. Difference between ARPEGE simulations and ERA-I mean SLP for the reference period 1981-2010 in winter (JJA) and summer (DJF). Value of the RMSE are given below the plots.

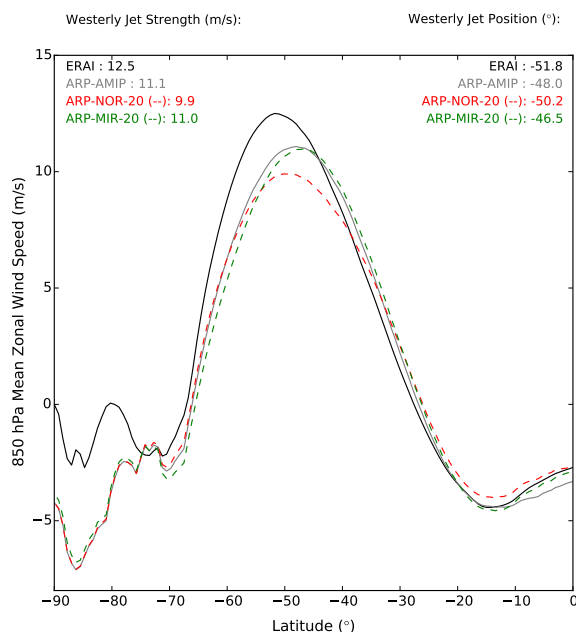


Figure 3. Mean latitudinal profile of 850 hPa Eastwards wind component (reference period : 1981-2010) for ARP-AMIP (grey), ARP-MIR-20 (dashed green), ARP-NOR-20 (dashed red) and ERA-Interim (black). Upper left : yearly mean strength (m/s), Upper right : latitude (°), of the westerlies wind maximum or "jet".

West Antarctic Ice Sheet (WAIS) in summer. Except for some coastal stations of East Antarctica, T_{2m} error in the ARP-AMIP simulation are very similar in the comparisons with MAR-ERA-I and READER data base.

Considering errors on surface temperatures of the Antarctic Plateau as large as 3 to 6K for ERA-I reanalysis in all seasons (Fréville et al., 2014), the magnitude of the errors in this region in ARP-AMIP simulation is encouraging. The error for Amundsen Scott station is even insignificant at $p=0.05$ level in all seasons but autumn (MAM). The warm bias on the large ice-shelves is due to the fact that ice-shelves are not considered as land in the ARPEGE version used. In order to correct this weakness, we prescribed an SIC of 100% and a thickness of 40 m in grid points corresponding to ice-shelves. Even if this reduced the initial bias by about 5K, it did not prevent the warm bias from still being as high as 12K in the center of the Ross Ice-Shelf in Winter. Part of the errors on this ice-shelf are also likely due atmospheric general circulation errors, but this issue will require further investigation. As a consequence of these large biases in temperatures and surface climate over large ice-shelves, surface mass balance and temperatures changes at the continent scale are only presented and discussed for the grounded ice sheet (GIS).

The large negative bias that ARP-AMIP shows for some coastal stations of East Antarctica (Casey, Davis, Mawson, Mc Murdo), especially in winter, are likely partly due to site-effects. First, ARPEGE temperatures are representative for a 40x40 km² inland grid point, whereas many weather stations are located very close to the shoreline. Second, ARPEGE underestimates

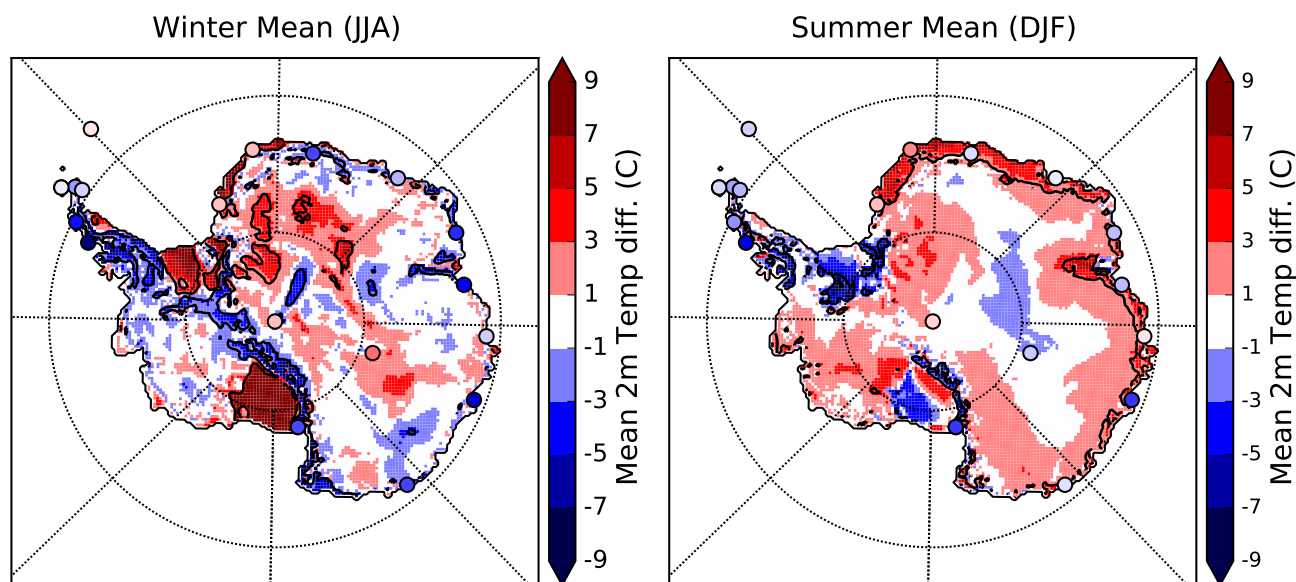


Figure 4. T_{2m} differences between ARP-AMIP and MAR-ERA-I simulations in winter (JJA, left) and summer (DJF, right) for the reference period 1981-2010. Circles are T_{2m} differences between ARP-AMIP and weather stations from the READER data base. Black contour lines represent areas where $|ARPEGE - MAR| > 1.5MAR\sigma$.

10m wind-speed in these stations in winter. An underestimate of the strength and frequency of katabatic winds reduces the adiabatic heating of the air masses flowing down from the Plateau to the coasts and favors the stratification of the air masses in these areas. Finally, a large cold bias at Rothera station on the Antarctic Peninsula is likely a combination of site effect and errors on atmospheric general circulation.

- 5 Regarding T_{2m} in ARPEGE simulations forced by NorESM1-M and MIROC-ESM historical SSC, the skills of ARPEGE model are particularly decreased over the AP and over the EAP to a lesser extent (see Fig. B2). Over coastal East Antarctic stations, most of the errors in T_{2m} are likely due to site-scale effects, topography differences or inadequacies of the physics of the atmospheric model and the skills of the atmospheric model shows few variations in the three simulations. The use of SSC from NorESM1-M and MIROC-ESM instead of observed SSC also leads to modified temperatures at the continental scale.
- 10 Differences for ARP-NOR-20 and ARP-MIR-20 in T_{2m} for the Antarctic GIS with respect to the ARP-AMIP simulation are presented in Tab. 4. For the ARP-MIR-20, differences of -0.7K in spring and -1.5K in Summer were found significant at $p=0.05$ level. For the ARP-NOR-20, differences ranging from 0,4K to 1,2K in autumn, winter and spring are significant as well.



Table 3. Error on READER weather station T_{2m} in the ARP-AMIP simulation for the reference period 1981-2010. Errors significant at $p=0.05$ are presented in **bold**.

Stations	DJF	MAM	JJA	SON
<i>EAP</i>				
Amundsen Scott	0.5	2.4	1.1	0.9
Vostok	-1.5	3.2	3.2	1.9
Mean error	-0.5	2.8	2.1	1.4
RMSE	1.1	2.8	2.4	1.5
<i>Coastal EA</i>				
Casey	-3.9	-5.7	-6.9	-5.4
Davis	-1.6	-4.2	-5.9	-3.3
Dumont Durville	-0.5	-2.8	-4.1	-2.2
Mawson	-2.2	-4.3	-5.7	4.3
McMurdo	-7.1	-6.5	-8.1	-8.4
Mirny	-1.2	-2.2	-3.0	-2.0
Novolazarevskaya	2.5	0.6	-1.0	0.6
Scott Base	-5.0	-3.2	-4.5	-5.0
Syowa	-0.2	-0.6	-1.5	0.0
Mean error	-2.1	-3.3	-4.5	-3.3
RMSE	3.4	3.8	5.0	4.2
<i>Ice shelves</i>				
Halley	1.2	2.4	1.2	0.8
Neumayer	2.1	1.2	0.9	1.4
Mean error	1.7	1.8	1.0	1.1
RMSE	1.7	1.9	1.0	1.1
<i>Peninsula</i>				
Bellingshausen	-1.0	-0.4	-0.2	-0.0
Esperanza	-1.1	0.5	-1.3	-0.8
Faraday	-2.6	-4.6	-5.7	-3.6
Marambio	-1.8	1.0	-1.3	-1.6
Marsh	-0.8	-0.3	-0.3	-0.0
Orcadas	-1.1	-0.0	0.6	-0.7
Rothera	-5.5	-7.9	-8.7	-6.1
Mean error	-2.0	-1.7	-2.4	-1.9
RMSE	2.5	3.5	4.0	2.8
<i>Southern Ocean</i>				
Gough	-1.0	-0.34	0.02	-0.79
Macquarie	-0.7	-0.4	0.2	-0.4
Marion	-1.2	-0.4	-0.0	-0.7
Mean error	-0.9	-0.4	0.1	-0.6
RMSE	0.9	0.4	0.1	0.7

Table 4. Mean seasonal T_{2m} differences for the GIS with respect to the ARP-AMIP simulation. Differences significant at $p=0.05$ are presented in **bold**.

Simulations	DJF	MAM	JJA	SON
ARP-NOR-20	-0.09	0.41	1.16	0.95
ARP-MIR-20	-1.48	-0.22	0.25	-0.65



3.1.3 Surface Mass Balance

In this study, SMB from ARPEGE simulations is defined as the total precipitation minus the surface snow sublimation/evaporation minus run-off. Differences between ARP-AMIP and MAR-ERA-I total precipitation, snow sublimation and SMB (in mm of water equivalent per year) for the reference period 1981-2010 can be seen in Fig. 5. As differences in run-off are restricted to the ice-shelves and some very localized coastal areas, their spatial distribution is not displayed in this figure. Yearly mean SMB, total precipitation, surface sublimation, run-off, rainfall and melt, integrated over the whole Antarctic GIS for the different ARPEGE simulations, for MAR-ERA-I and from other studies are presented in Table 5.

At the continental scale, we can see that estimates of the SMB of the ice-sheet from the ARP-AMIP simulation resemble those from state of the art polar-oriented RCM MAR and RACMO2. However, higher total precipitation values in ARPEGE-AMIP are compensated for by much higher values of sublimation/evaporation of surface snow and, to a lesser extent, higher run-off. Total precipitation in ARP-AMIP simulation is 274 Gt yr^{-1} higher than in the MAR-ERA-I simulation, corresponding to about 2.8 interannual standard deviations (σ). Precipitation is generally higher in ARPEGE over most of the coastal areas. The largest precipitation overestimates with respect to MAR are found in the Ross sector of Marie-Byrd Land, in Dronning Maud and Coats Land and in the Northern and Eastern part of the Antarctic Peninsula. On the other hand, precipitation is lower in ARP-AMIP in the Southern and Western part of the Peninsula, in the inland part of central WAIS and in the interior and lee-side of the Transantarctic Mountains. Sublimation/evaporation of snow integrated over the whole ice-sheet is about four times higher in ARP-AMIP than in MAR-ERA-I. Differences mostly come from coastal areas and the lower slopes of the ice-sheet. This is consistent with ARP-AMIP being systematically 1 to 3K warmer than MAR-ERA-I in summer in those areas. Run-off at the continent scale is eight times higher in ARP-AMIP than in MAR-ERA-I, which is also most likely a consequence of warmer coastal areas in ARPEGE in summer. However, inter-annual variability is very high in the simulated ARPEGE run-off, and so it is in MAR-ERA-I (σ is at least 50% of the mean). If we have a closer look at the values of rainfall, surface snow melt and run-offs in the three present-day ARPEGE simulations in Table 5, the ratio between inputs of liquid water into the snow pack (rainfall + surface snow melt) and the water run-off that finally leaves the snow-pack is about 1/4. In MAR-ERA-I and in RACMO2-ERA-I, this ratio is about 1/20. This means that although the snow surface scheme SURFEX-ISBA used in ARPEGE is able to model storage and refreezing of liquid water in the snow-pack, the retention capacity of the Antarctic snow pack underestimated with respect to MAR and RACMO2.

In ARP-MIR-20 simulation, snow sublimation and evaporation, run-off and melt were found significantly lower than in ARP-AMIP, which is consistent with this simulation being 1.5K cooler in summer (DJF). The effect of driving ARPEGE by biased SSC for the modelling of Antarctic precipitation is discussed in the supplementary material (see Sec. C).

3.2 Climate change signal

In this section, we present the climate change signal obtained for the RCP8.5 scenarios coming from NorESM1-M and MIROC-ESM SSC. For ARPEGE scenarios realized using original SSC from the two coupled models (ARP-NOR-21 and ARP-MIR-21), the reference simulations for the historical period are the ARPEGE simulations performed with historical SSC coming

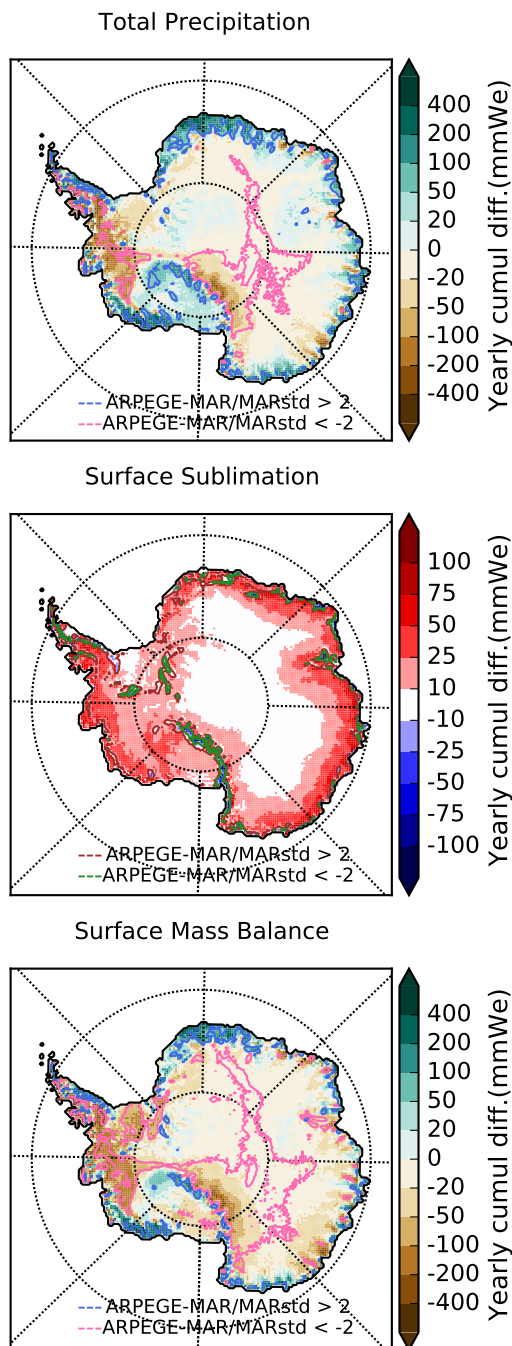


Figure 5. Total Precipitations (*top*), Sublimation/Evaporation (*centre*) and Surface Mass Balance (*bottom*) for ARP-AMIP minus MAR-ERA-I yearly cumul difference (mmWe.yr^{-1}) for the reference period 1981-2010. Pink (brown) and blue (green) contour lines represents areas where ARPEGE-MAR differences are respectively smaller than -2 or bigger than 2 MAR standard deviation of annual values (2σ).



Simulation	SMB	Tot. PCP	Surf Subl.	Run-Off	Rainfall	Melt
ARP-AMIP	2192±107	2529±105	316±19	21±13	11±2	55±34
ARP-NOR-20	2436±112	2771±111	314±14	20±11	11±2	56±29
ARP-MIR-20	2228±94	2532±103	294±21	10±6	10±2	31±19
MAR-ERA-I ¹	2125±104	2204±100	79±9	0.5±0.5	12±2	34±11
RACMO2-ERA-I ¹	2085±91	2213±97	128±3	1±1	2±1	46±16
RACMO2-ERA-I ² (entire ice sheet)	2596±121	2835±122	228±11	5±2	6±2	88±24
CESM-hist ³	2280±131	2433±135	68±6	86±21	5±2	203±41
(Vaughan et al., 1999)	1811					

Table 5. Mean Grounded Antarctic Ice-Sheet Surface Mass Balance and its component (Gt yr^{-1}) \pm one standard deviation of the annual value for the reference period 1981-2010. Variables from ARP-NOR-20 and ARP-MIR-20 that are significantly different from the value in ARP-AMIP at $p=0.05$ level are in bold. ¹MAR and RACMO2 forced by ERA-I statistics for 1981-2010 for Antarctic GIS using the same ice-masks such as in Agosta et al. (2018), sublimation values for RACMO2 include drifting snow sublimation. ²RACMO2 statistics are given for the total Ice-Sheet and the period 1979-2005 from Lenaerts et al. (2016), sublimation includes drifting snow sublimation. ³Community Earth System Model historical simulation (1979-2005), values for the total ice-sheet from Lenaerts et al. (2016)

from the respective coupled model (ARP-NOR-20 and ARP-MIR-20). For scenarios realized with bias correction of the SSC (ARP-NOR-21-OC and ARP-MIR-21-OC), the reference simulation for the historical period is ARP-AMIP (observed SSC). The primary goal here is to evaluate the uncertainty in climate change signals for Antarctica associated with oceanic forcing coming from coupled models and the changes coming from the bias correction of the SSC.

5 3.2.1 Atmospheric General Circulation

Climate change signals in mean SLP for the different RCP8.5 scenarios realized with ARPEGE can be seen in Fig. 6. All scenarios show a pressure increase at mid-latitudes (30-50°S) and a decrease around Antarctica. This corresponds to a shift of the circum-antarctic low pressure belt towards the continent (positive phase of the SAM) and is a generally expected consequence of 21st century climate forcing (Kushner et al., 2001; Arblaster and Meehl, 2006). This pattern (increase at mid-latitude, decrease around Antarctica) is sharper in scenarios realized with MIROC-ESM SSC.

Differences in the climate change signal for ARP-NOR-21-OC and in ARP-NOR-21 with respect to their corresponding references in historical climate are small. The ASL deepens more in the scenario realized with non bias-corrected SSC (ARP-NOR-21) in winter while it is the opposite in summer. Differences in SLP climate change signal are more obvious in the scenarios realized with MIROC-ESM SSC. In the scenario realized with non bias-corrected SSC (ARP-MIR-21), the intensification of the low pressure systems around Antarctica in winter is clearly organized in a 3-wave pattern (Fig. 6b). In ARP-MIR-21-OC, the JJA pressure decrease is rather organized in a dipole with one maximum of pressure decrease centered the Eastern side of the Ross Sea and another one West of the Weddell Sea. As a result, the 3-wave pattern is clearly noticeable in the difference between the two scenarios climate change signals (Fig. 6b, right). In summer, the differences between the two simulations are



Table 6. Changes in mean yearly Southern westerly wind maximum or "jet" strength (Δ WMSTR, m/s) and position (Δ WMPOS, °) for the different ARPEGE scenarios

Simulations	Δ WMSTR (m/s)	Δ WMPOS (°)
ARP-NOR-21	1.7	-0.8
ARP-NOR-21-OC	1.5	-2.2
ARP-MIR-21	1.9	-3.7
ARP-MIR-21-OC	2.0	-3.8

weaker and mainly consist of a sharper pressure increase at mid latitudes in ARP-MIR-21-OC.

Regarding the changes in westerly wind maximum strength (Table 6), the differences between the two scenarios using NorESM1-M SSC are once again limited. We can however mention a -1.4° higher decrease in westerly winds maximum position in the scenario using bias-corrected SSC. Differences in changes in position and strength are not substantial between ARP-MIR-21 and APR-MIR-21-OC. Compared to scenarios realized with SSC from NorESM1-M, these scenarios show a slightly larger increase in jet strength and a much larger poleward shift, although this difference is reduced when comparing scenarios with bias corrected SSC.

3.2.2 Near-surface Temperatures

The mean yearly T_{2m} increase for the Antarctic GIS using SSC from NorESM1-M rcp8.5 scenario is 2.9 ± 1.0 K using original SSC (ARP-NOR-21) and 2.8 ± 0.8 K using bias-corrected SSC (ARP-NOR-21-OC). For scenarios using SSC from MIROC-ESM, these temperatures increases are respectively 3.8 ± 0.7 K and 4.2 ± 1.0 K. The differences in yearly T_{2m} increase using bias-corrected SSC are found non significant at $p=0.05$ level in both cases. T_{2m} increase per season can be seen in Tab. 7. Only a $+0.8$ K difference in winter temperature increase in ARP-MIR-21-OC with respect to the scenario with original SSC is found significant. At the regional scale (Fig. 7b), this is materialized by large areas of 1 to 2K stronger warming in the centre of the East Antarctic Plateau, Dronning Maud Land, Byrd Land, and the Ross ice shelf. The difference in warming in ARP-MIR-21-OC is the highest in Marie-Byrd Land ($+2$ K).

For scenarios using SSC from NorESM1-M, no seasonal difference was found significant at the scale of the ice-sheet although a 0.5 K weaker temperature increase in summer for ARP-NOR-21 is close to the significance threshold. However, if we look at regional warming (Fig. 7a), we can see that for large areas covering the center of East Antarctic Plateau and coastal areas, the regional warming is 0.5 to 1 K higher in winter and 0.5 to 1 K lower in summer in the scenario with bias-corrected SSC.

3.2.3 Precipitations and Surface Mass Balance

Statistics of SMB and its component for the reference period 2071-2100 at the scale of the Antarctic GIS are presented in Tab. 8. For the experiment realized with NorESM1-M SSC, precipitation and SMB changes (in both cases increases) are very similar, while there is about 250 Gt.yr^{-1} more precipitation and therefore accumulation in ARP-NOR-21 absolute values.

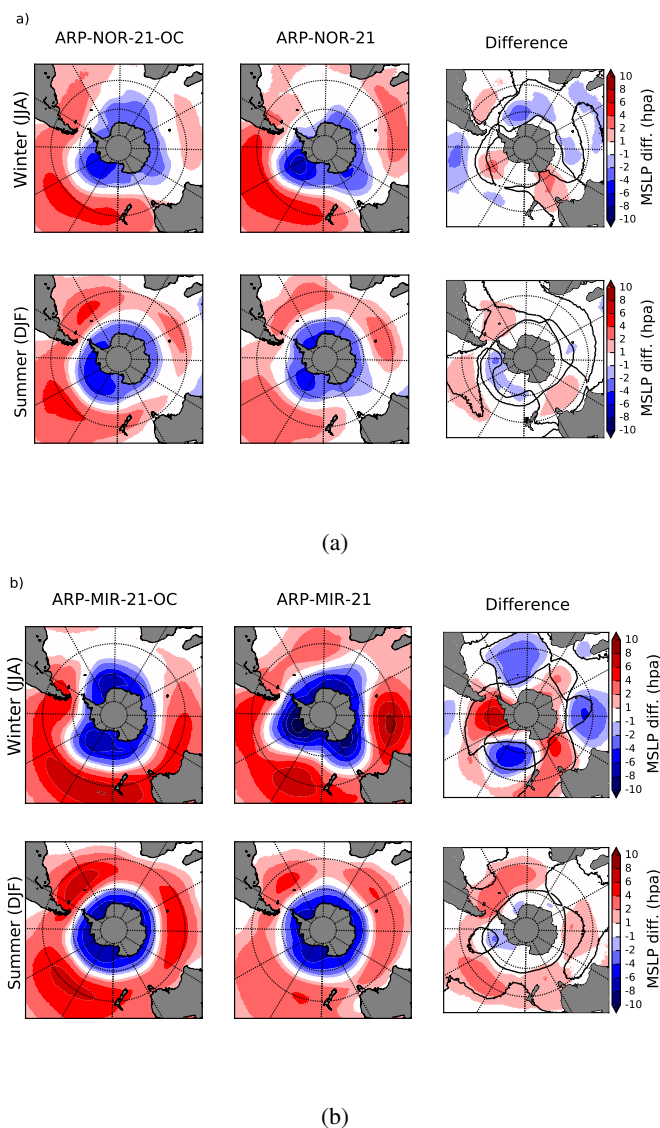


Figure 6. Climate change signal in SLP for ARPEGE RCP8.5 scenarios with bias corrected SSC (*left*), original SSC (*center*) and difference (*right*). Climate change signal for winter (JJA) are displayed at the *top* of the subfigures and for summer (DJF) at the *bottom*. Results for scenarios with SSC from NorESM1-M are presented in subfigure (a) and from MIROC-ESM in subfigure (b). *Black contour lines* represent areas where differences in climate signal is 50% of the climate signal in the simulation with non bias-corrected SSC.

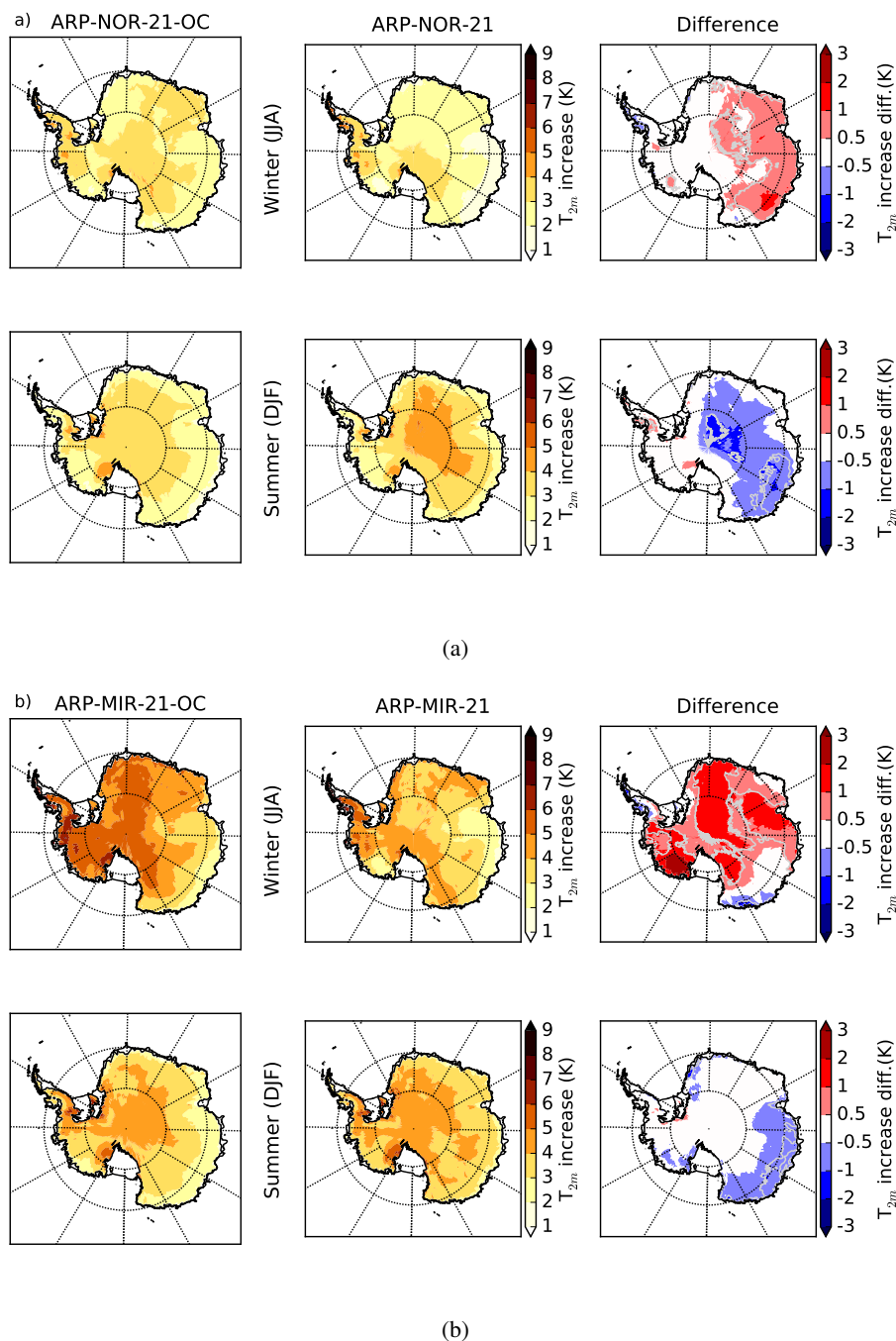


Figure 7. Climate change signal in T_{2m} for ARPEGE RCP8.5 scenarios at the end of the 21st (reference period : 2071-2100) with bias corrected SSC (left), original SSC (center) and difference (right). Climate change signal for winter (JJA) are displayed at the top of the subfigures and for summer (DJF) at the bottom. Results for scenarios with SSC from NorESM1-M are presented in subfigure (a) and from MIROC-ESM in subfigure (b). Grey contour lines is where differences in climate change signal is 25% of the climate change signal using non bias corrected SSC



Table 7. Mean season T_{2m} increase (K) for the Antarctic GIS for the different ARPEGE RCP8.5 scenario at the end of 21st (reference period: 2071-2100) with respect to their historical reference simulation (reference period: 2071-2100). Climate change signal in scenarios with bias-corrected SSC significantly different at $p=0.05$ level are presented in bold.

Simulations	DJF	MAM	JJA	SON
ARP-NOR-21	3.5±1.4	2.7±1.4	2.6±2.0	2.7±1.4
ARP-NOR-21-OC	3.0±1.4	2.6±1.4	3.1±1.4	2.6±1.0
ARP-MIR-21	3.9±0.9	4.1±1.3	3.8±1.4	3.5±1.2
ARP-MIR-21-OC	3.6±1.5	4.6±1.7	4.6±1.4	3.8±1.5

For both total precipitation and SMB, absolute values were found significantly different at $p=0.05$ level in ARP-NOR-21-OC with respect to ARP-NOR-21, while climate changes signals were not. No significant difference in absolute values or climate change signals were found for the other components of SMB for scenarios with NorESM1-M SSC.

For scenarios performed with MIROC-ESM SSC, absolute values and increase in precipitations are about 185 Gt.yr⁻¹ stronger in the scenario with bias-corrected SSC. The difference in SMB between the two scenarios is slightly reduced by a larger run-off in ARP-MIR-21-OC simulation. The total precipitation increase is as high as +8.8% K⁻¹ in ARP-MIR-21-OC, compared to a 6.1% K⁻¹ increase in ARP-MIR-21. For SMB and precipitations, both absolute values and climate changes signals were found significantly different in ARP-MIR-21-OC than in ARP-MIR-21. As for the ARP-MIR-20 reference, absolute value in yearly run-off is found significantly different than in the corresponding non bias-corrected simulation.

In each scenario, the sublimation increases by about 20 to 25% with respect to the corresponding references in the historical period. Run-off and melt increase by about a factor 4 in scenarios with NorESM1-M SSC and by factors ranging from 6 to 10 in scenarios with MIROC-ESM SSC. This, however, does not prevent these components to remain one order of magnitude smaller than total precipitation. As a consequence, increases in SMB are essentially determined by the increases in total precipitation. In future climate simulated by ARPEGE, the ratio between liquid water inputs (rainfall + melt) and liquid water leaving the snow-pack (run-off) remains around 1/3. As the change in SMB is mainly the result of change in total precipitation, we only present here the spatial distribution of changes in precipitation in Antarctica in Fig. 8. In all scenarios, the strongest absolute precipitation increases occur in the coastal regions of West Antarctica and in the West of the Peninsula. In simulations with MIROC-ESM SSC, precipitation increase is also very strong in the Atlantic sector of coastal East Antarctica. The difference between total precipitation increases in ARP-NOR-21 and ARP-NOR-21-OC (Fig. 8a) is small in most regions of Antarctica, except for a stronger increase (or lower decrease) in Marie-Byrd Land, and a lower increase in Adélie Land in ARP-NOR-21-OC. For the simulations with MIROC-ESM SSC (Fig. 8b), we can clearly identify an alternation of three regions of higher or lower precipitation increases. This tri-pole pattern can easily be linked with the 3-wave pattern in SLP change in ARP-MIR-21, clearly different than the pattern in MSLP change in ARP-MIR-21-OC (Fig. 6b). Here again, Marie Byrd Land and Adélie Land are among the areas where large differences are found between simulations with or without bias-corrected SSC. Here, substantial differences are also found in Dronning Maud and Wilkes Land, as well as on the western flank of the East Antarctic Plateau, south of Dronning Maud Land. Winter and spring (and to a lesser extent autumn) are the seasons mostly responsible for



Table 8. Absolute value, absolute and relative climate change signal for Mean SMB and components ($Gt\ yr^{-1}$) for the Antarctic GIS for the different ARPEGE RCP8.5 scenario (reference period: 2071-2100). Climate change signals and absolute values significantly different at $p=0.05$ level in scenarios with bias-corrected SSC are displayed in bold.

Simulations	SMB	Tot. PCP	Surf. Sublim.	Run-Off	Rainfall	Melt
ARP-NOR-21	2817±156	3311±185	386±32	107±46	29±7	260±136
<i>CC change ($Gt\ yr^{-1}$)</i>	381±211	540±220	72±29	86±38	17±8	203±114
<i>Rel. change</i>	16%	20%	23%	423%	152%	360%
ARP-NOR-21-OC	2585±201	3060±196	377±24	99±41	29±7	241±120
<i>CC change ($Gt\ yr^{-1}$)</i>	393±209	531±200	60±28	78±35	18±8	1856±94
<i>Rel. change</i>	18%	21%	19%	379%	161%	336%
ARP-MIR-21	2784±109	3288±145	378±27	126±51	49±13	321±156
<i>CC change ($Gt\ yr^{-1}$)</i>	556±143	756±152	84±20	116±46	39±13	290±140
<i>Rel. change</i>	25%	30%	20%	1170%	381%	936%
ARP-MIR-21-OC	2914±172	3469±224	392±33	162±63	54±16	403±190
<i>CC change ($Gt\ yr^{-1}$)</i>	723±219	940±254	76±26	142±54	43±15	347±161
<i>Rel. change</i>	33%	37%	24%	688%	386%	627%

differences in precipitation changes between the simulations with MIROC-ESM original SSC. The relative mean precipitation changes (in%) and associated standard deviation for four RCP8.5 scenarios realized in this study can be seen in Fig. 9.

4 Discussion

4.1 Reconstruction of the historical climate

- 5 The atmospheric model ARPEGE correctly captures the main features of the atmospheric circulation around Antarctica. The three local minima in SLP and 500hPa geopotential, generally present around 60°W, 90°E and 180 °E, are well reproduced in the ARPEGE-amip simulation (see Fig. D1a). However, there is a positive SLP bias in the seas around Antarctica, particularly in the ASL sector, and a negative bias in mid-latitudes (30-40°S), especially in the Pacific sector. This bias structure in the Southern Hemisphere is present in many coupled and atmosphere-only GCMs. Its consequence is an equator-ward bias in
- 10 the position of the surface jet associated with westerly winds (Bracegirdle et al., 2013). The use of observed SSC (ARP-AMIP) rather than SSC from NorESM1-M and MIROC-ESM substantially improves the simulated mean SLP in the Southern Hemisphere in all seasons but summer. This confirms results from previous studies which have shown that the use of observed rather than modeled SSC to drive atmosphere-only model clearly improves the skill of the atmospheric models (Krinner et al., 2008; Ashfaq et al., 2011; Hernández-Díaz et al., 2017). In ARP-NOR-20, the use of modeled SSC yields a better comparison
- 15 with ERA-I in terms of westerly winds maximum position while its strength is much largely underestimated. In ARP-MIR-20, the strength of the westerlies maximum is similar to ARP-AMIP, but the equatorward bias on the position is much larger. The

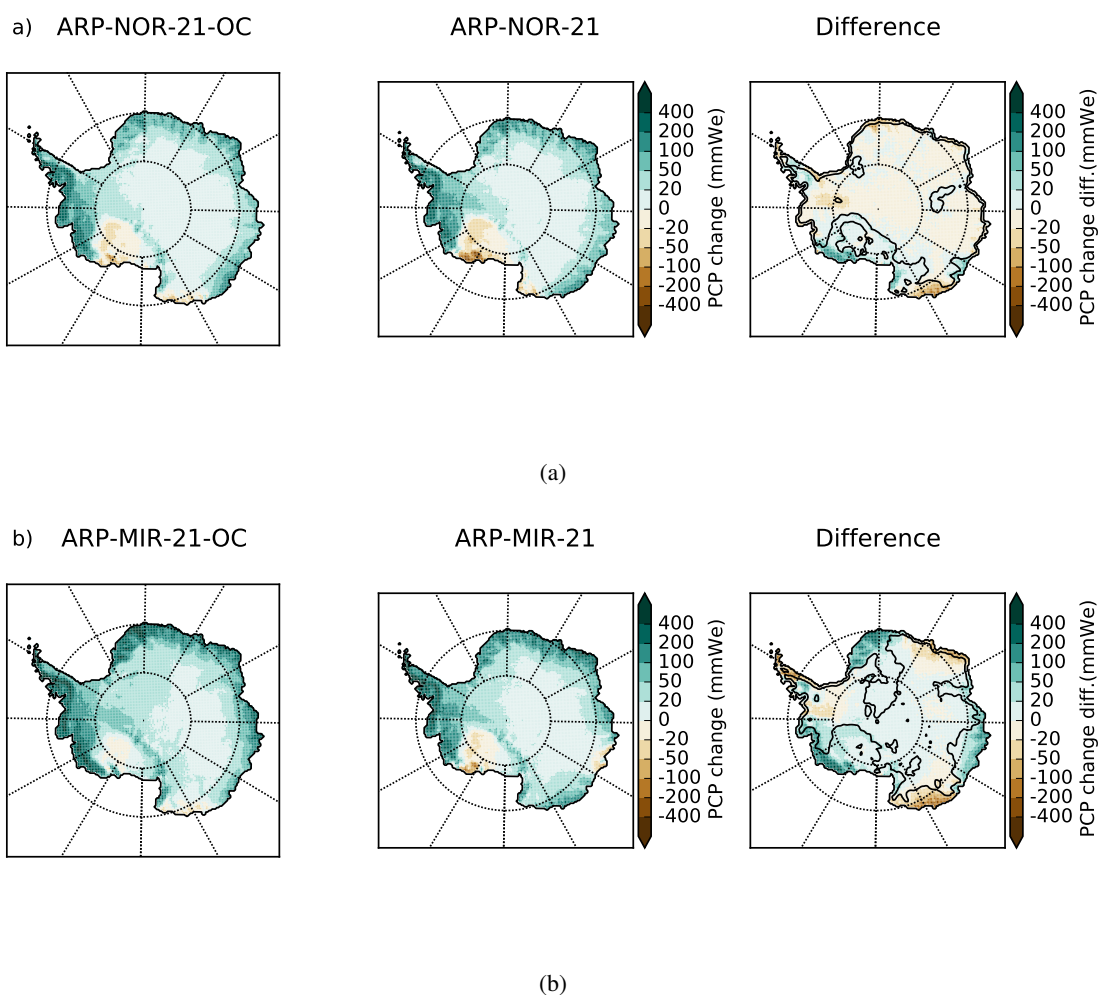


Figure 8. Climate change signal in Total Precipitations at the end of the 21st century (reference period: 2071-2100) for ARPEGE RCP8.5 scenarios with bias corrected SSC (*left*), original SSC (*center*) and difference (*right*). Results for scenarios with SSC from NorESM1-M are presented in subfigure (a) and from MIROC-ESM in subfigure (b). Black contour line indicates where difference is 50% of the precipitation change in the non bias-corrected SSC scenario.

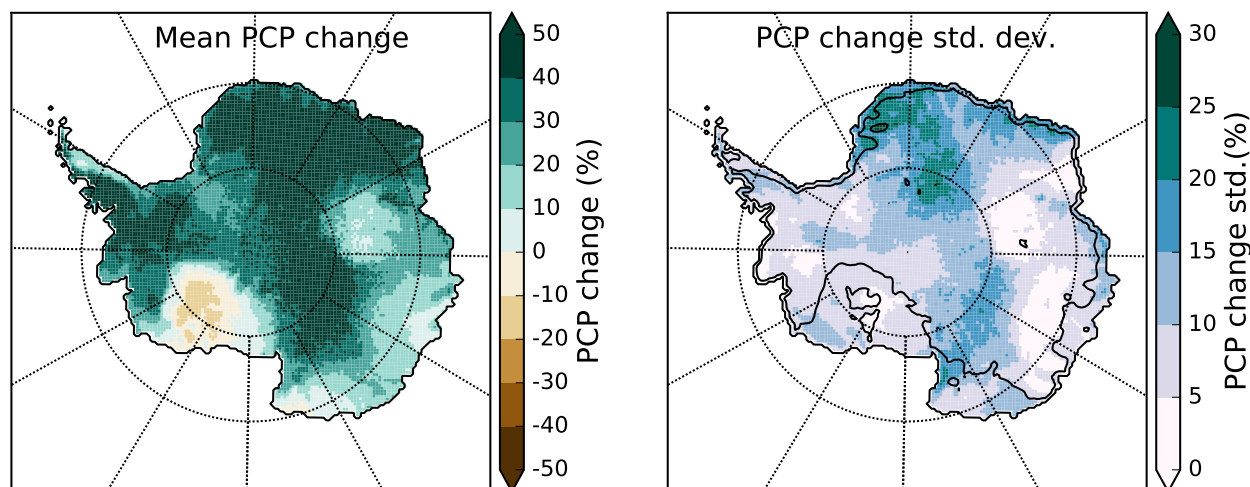


Figure 9. Mean (left) relative precipitation change (%) for late 21st century from the four ARPEGE RCP8.5 scenario and associated standard deviation (right). Black contour line indicates where standard deviation is 50% of the mean change.

equatorward bias found in the 850hPa westerly wind maximum position ($\sim 3^\circ$) in ARP-AMIP is very similar to the bias found by Bracegirdle et al. (2013) for the surface westerly wind maximum in CMIP5 and AMIP simulation from CNRM.

Regarding surface climate, ARPEGE also correctly reproduces Antarctic T_{2m} except over the large ice-shelves. The T_{2m} error with respect to MAR is generally lower than 3K over most of the GIS. There is a warm bias on the ridge of the Antarctic Plateau in winter. However, the magnitude of these errors (+1.5K at Amundsen-Scott, +3.4K at Vostok) is to be compared with much larger biases in other GCMs or even in reanalysis, as most models usually fail to capture the strength of the near-surface temperature inversion. The cold bias of ARPEGE on the Antarctic Peninsula, especially in winter, can largely be explained by atmospheric circulation errors, as an underestimate of the depth and/or recurrence of the ASL leads to an underestimate of mild and moist flux from the North-West onto the Peninsula.

10 The GIS SMB in ARP-AMIP simulation ($2191 \pm 106 \text{ Gt yr}^{-1}$) falls within the 1-standard deviation (1σ) uncertainty range with respect to estimates using the MAR RCM, and concurs with studies using other RCMs and GCMs or independent estimates. However, it has to be mentioned that higher precipitation rates in the ARP-AMIP simulation than in MAR and RACMO2 (about 2.5σ) are compensated for by a much stronger surface snow sublimation in the ARPEGE simulations. Some of the differences with MAR-ERA-I in the spatial distribution of precipitation rates in the ARP-AMIP simulation can also be linked to errors in atmospheric general circulations. These errors are certainly part of the explanation for ARPEGE being wetter in Marie-Byrd Land, in the Eastern and Northern part of the Peninsula and in Dronning Maud Land as well as for ARPEGE being drier in central West Antarctica and in the western part of the Peninsula.

When forced by SSC from NorESM1-M, ARPEGE simulated significantly higher precipitation rates at the scale of the ice-



sheet (+243 Gt yr⁻¹, 2.3σ). When forced by MIROC-ESM SSC, run-off and snow sublimation were found significantly lower due to cooler temperatures in spring and summer.

4.2 Climate change signals

As described above, NorESM1-M and MIROC-ESM have been chosen because they display very different RCP8.5 scenarios in terms of change in sea-ice around Antarctica by the end of the 21st century. Indeed, these two models suggest a decrease of respectively -14% and -45% of winter SIE around Antarctica between 1091-2010 and 2071-2100.

For the RCP8.5 simulation using SSC from NorESM1-M, the use of bias-corrected SSC has not yielded significantly different climate change signals with respect to the simulation using uncorrected SSC. The changes in SLP and 850hPa westerlies maximum strength are very similar in both cases and so is the increase in mean annual temperature (around 2.8±1K). The T_{2m} changes are not significantly different in any season, and neither are changes of SMB and its individual components. For future scenarios with SSC from MIROC-ESM, the use of bias-corrected SSC induced a significantly different climate change signals for most variables, especially in winter. In the scenario with original MIROC-ESM SSC, the deepening of the low pressure zone around Antarctica is mainly organized in a three-wave pattern in JJA. In the scenario with bias-corrected SSC, this SLP decrease is rather organized following a dipole. These differences in changes in atmospheric general circulation have yielded significantly different changes in atmospheric temperatures (0.8K greater in ARP-MIR-21-OC in winter), the most dramatic difference being a 2K bigger increase in west Marie-Byrd Land using bias corrected SSC. Differences in atmospheric circulation are also unsurprisingly associated with significantly different changes in total precipitation (and SMB). At the continent scale, the increase in moisture advection approximated trough P-E is 9% larger in ARP-MIR-21-OC than in ARP-MIR-21. The consequences of the three-wave pattern in ARP-MIR-21 decrease in SLP around Antarctica are obvious with three regions of higher (lower) precipitations increases with respect to the ARP-MIR-21-OC scenario. At the regional scale, it is noteworthy that all scenarios agree on a (slight) precipitation decrease in Marie-Byrd Land and western Ross ice shelf (see Fig. 9). Victoria, Adélie, and Wilkes Land as well as the eastern side of the AP are also regions of lower precipitation increase compared to the rest of the continent. All these regions show high uncertainty in future changes in precipitation estimated in this study (Fig. 9, high value of standard deviation when compared to mean change). Lower increase or slight decrease in precipitation in Marie-Byrd Land are also present in other studies (Krinner et al., 2008; Lenaerts et al., 2016). These results however bear uncertainties as lot of free AGCM (including ARPEGE) struggle to reproduce the depth and the variability of the Amundsen Sea Low currently located at the east side of the Ross Sea in winter. The decrease in precipitation in this region is mitigated when using both set of bias corrected SSC.

The increase in annual mean T_{2m} at the end of the 21st century for the Antarctic ice-sheet with the different ARPEGE scenarios are in good agreement with the CMIP5 RCP8.5 outputs (Palermé et al., 2017). Unsurprisingly, the warming obtained with scenarios using SSC from NorESM1-M (around +2.8K) belongs to the lower end of the values for RCP8.5 scenario reported in this previous study, as a consequence of weak changes in Antarctic sea-ice in this projection, whereas in scenarios using MIROC-ESM SSC, the increase in annual T_{2m} is around +4K. As suggested by Krinner et al. (2010), the choice of the AOGCM providing SSC is determinant in the warming obtained at the Antarctic-continent scale. Using NorESM1-M and original SSC



from MIROC-ESM, the SMB (precipitation) increase obtained with ARPEGE range between 5.2 and 6.3 $\% \cdot K^{-1}$ (6 and 7.4 $\% \cdot K^{-1}$). This is in the range of values obtained in previous studies (Agosta et al., 2013; Ligtenberg et al., 2013; Krinner et al., 2014; Frieler et al., 2015; Palerme et al., 2017). Only the SMB increase obtained with bias-corrected SSC from MIROC-ESM, 7.9 $\% \cdot K^{-1}$ is above the higher end values of previous studies. As in Krinner et al. (2014), we found that regional precipitation increases depend on the AOGCM chosen as SSC source and on their bias-correction or not. For a weaker climate change signal such as the one coming from NorESM1-M SSC, we found no significant difference in climate change signals at the continent scale over Antarctica using bias corrected or original SSC to drive ARPEGE. However, for a more dramatic change in SSC such as the one coming from MIROC-ESM, we found a +14% higher precipitation increase using bias-corrected SSC. Finally, we draw the attention on the fact that when considering absolute values rather than climate change signals, both annual total precipitation rates and SMB are significantly different than when using bias corrected SSC. In the scenarios with original SSC, the annual GIS SMB at the end of current century is slightly higher in ARP-NOR-21 than in ARP-MIR-21, which is a bit surprising considering the very weak decrease in sea-ice around Antarctica in NorESM1-M RCP8.5 scenario. When using bias-corrected SSC, the order is reversed and SMB values are respectively 2585 $Gt \text{ yr}^{-1}$ and 2914 $Gt \text{ yr}^{-1}$, which is more intuitive considering much larger decrease in sea-ice in MIROC-ESM RCP8.5 scenario.

15 4.3 Consistency of atmospheric model responses

The late winter (ASO) and late summer (FMA) differences between historical SST and SIC from NorESM1-M and MIROC-ESM and the observations, as well as the same differences between SSC of their RCP8.5 scenario and their bias-corrected equivalent are displayed in the annex (Fig. A1 and A2). The differences in SSC used to drive the atmospheric model are, unsurprisingly, extremely similar between historical and future climate experiments. For the SST, the similarity is almost perfect and for SIC, the patterns are the same, but given the decrease in SIC in future climate, they are shifted poleward.

Has the introduction of the same SSC “biases” with respect to the observed or bias-corrected references yielded the same responses of the atmospheric model in the historical and future climates? This consistency of the response of the atmospheric model is considered here as being the key for having the same climate change signals between experiments using original SSC from the CMIP5 model and experiments considering the climate change signal between the AMIP experiment and the corresponding bias-corrected projected SSC.

For simulations using SSC from the NorESM1-M model, the consistency of the response of the atmospheric model is obvious. The similarity in the differences between ARP-NOR-20 and ARP-AMIP with differences between ARP-NOR-21 and ARP-NOR-21-OC is strong for most climate variables, e.g. SLP, 500 hPa geopotentials, stratospheric temperatures, 500hPa zonal wind, near-surface atmospheric temperatures...(an example for SLP can be seen in Fig. D2). The most interesting feature in this perspective is that in both historical and future climate, the ARPEGE simulations forced by NorESM1-M original SSC are about 10% wetter and significantly warmer in winter and spring at the Antarctic continental scale than their bias-corrected reference. The link here between the dynamical response of the atmospheric model and the SST biases of the NorESM1-M AOGCM seems physically consistent. NorESM1-M SSTs are indeed characterized by a warm bias in Southern hemisphere mid-latitudes (40-60°S) and a cool bias in the Southern Tropics (except for large upwelling areas, see Fig. A3a), having as



a consequence a decrease of the meridional SST gradient. These biases are stronger in winter and spring. The response of the atmospheric model is here a decrease in the westerly winds (which is confirmed by a weaker surface westerly winds in the historical simulation), which allows an increase in the moisture transport towards Antarctica (P-E larger by about 10% in present and future climate) and explains the additional 200 to 300 Gt.yr⁻¹ (1.5 to 2 σ) of precipitation on the ice-sheet in the ARPEGE simulations realized with NorESM1-M SSC. The warm SST bias in the 40-60°S region, which is a large part of the moisture source region for Antarctic precipitation (Delaygue et al., 1999) is certainly also part of the explanation for larger precipitations. The consistency of the response of the atmospheric model in historical and future climate explains the absence of significant differences in the climate change signals between experiments with original NorESM1-M SSC and their bias-corrected reference.

For the simulations realized with oceanic forcings from MIROC-ESM, the consistency of the response of the atmospheric model is less generalized. Some changes in the differences between simulations forced with original SSC and those forced by their bias-corrected references are noticeable in winter and autumn SLP and zonal wind speed (an example for SLP can be seen in Fig. D3). The main result here, as a consequence of these differences, is a total precipitation difference in the RCP8.5 experiment with bias-corrected SSC of about +200 Gt yr⁻¹ (1 σ), while there was almost no difference in total precipitation in the historical period between ARP-AMIP and ARP-MIR-20. In both historical and RCP8.5 experiments, simulations with original SSC from MIROC-ESM model are cooler over most of Antarctica in spring and summer. Here, the link between biases in Southern Hemisphere SST from MIROC-ESM (see Fig. A3) and the response of ARPEGE appears less clear. SSTs from MIROC-ESM are mainly characterized by a cold bias at mid-latitudes and a warm bias around Antarctica, especially in summer and autumn, as well as a cold bias in the Tropics throughout the years. ARPEGE simulation forced by these SSTs are characterized by an equatorward surface westerly winds maximum in the historical simulation but not in the future scenario. Changes in the latitude of maximal SST gradient might explain the equatorward position of the westerlies maximum. However, with respect to ARP-AMIP simulation, ARP-MIR-20 is also characterized by cooler temperatures throughout the tropical troposphere, higher tropical stratospheric temperatures in spring and much lower upper tropospheric and stratospheric temperatures in Antarctica. This suggests that interactions between SST biases, tropical convection and stratospheric meridional temperature gradients could also explain the response of the atmospheric model when forced by MIROC-ESM SSC.

4.4 Implication of Sea Surface Conditions selection

In many cases, it has been reported that selecting best skilled models for a given aspect of the climate system helped in better constraining the associated uncertainties on climate change signal (e.g., Massonnet et al., 2012). Here, because we use bias-correction of the SSC, this aspect has reduced importance. Our aim is to cover as much as possible, while performing a limited number of climate projections, the range of uncertainties associated with the evolution of the Southern Ocean surface condition for the Antarctic climate projection as it was shown to be its primary driver (Krinner et al., 2014). The fact that biases on large-scale atmospheric circulation of coupled climate models were shown to be highly stationary under strong climate change (Krinner and Flanner, 2017) and that the response of ARPEGE atmospheric model to the introduction of the same SSC “bias” was shown to be mostly unchanged in future climate support this approach.



The warming signal for the Antarctic ice-sheet in the CMIP5 model ensemble RCP8.5 scenario is evaluated to be 4 ± 1 °C (Palermo et al., 2017). Interestingly, by picking NorESM1-M and MIROC-ESM which show some of the more opposite climate change signal on Southern Hemisphere SIE among the CMIP5 ensemble, we cover in our scenario (2.8 to 4.2 °C) mostly the lower half of this uncertainty range on Antarctic warming. Bracegirdle et al. (2015) found that about half of the variance of the CMIP5 projection in RCP8.5 scenario for Antarctic temperature and precipitation is explained by historical biases and sea-ice decrease by late 21st century. Obviously, a non negligible part of the uncertainties on Antarctic climate changes is linked to the representation of general circulation in the atmospheric model (Bracegirdle et al., 2013) and these should be assessed in future work.

5 Summary and Conclusion

In this study, we present a first general evaluation of the capability of the AGCM ARPEGE to reproduce the atmospheric general circulation and the surface climate of the Antarctic ice-sheet. ARPEGE is able to correctly represent the main features of atmospheric general circulation, although a negative bias in sea-level pressures at mid-latitudes and a positive bias around Antarctica especially in the Amundsen sector is to be reported. Unsurprisingly, the use of observed sea surface conditions (ARP-AMIP simulation) rather than SSC from NorESM1-M and MIROC-ESM helped to improve the representation of sea-level temperatures in the southern latitudes in all seasons but summer. ARPEGE is also able to correctly reproduce surface climate of Antarctica except for large ice-shelves. The differences in T_{2m} with polar RCM MAR and *in-situ* observations is encouraging, especially given the large biases that can exhibit other GCMs or even reanalysis when surface climate of Antarctica is considered (Fréville et al., 2014; Bracegirdle and Marshall, 2012). Regarding SMB, our estimates at the continental scale concur with estimates from other studies such as those using polar RCM MAR or RACMO2, even though higher precipitation rates in ARPEGE tend to be compensated for by higher surface snow sublimation rates ($+200 \text{ Gt yr}^{-1}$). Concerning regional patterns, the distribution of precipitation in ARP-AMIP simulation differs from the one in the MAR RCM, mainly as a consequence of errors in atmospheric general circulation.

Concerning climate change signals, we evaluate the impact of using original and bias-corrected sea surface conditions from MIROC-ESM and NorESM1-M, which display very different changes in winter SIE in their RCP8.5 scenario : respectively -45% and -14% at the end of the 21st century (2071-2100). Using SSC from NorESM1-M model, we found a T_{2m} increase of +2.8K and a precipitation increase of about 20%. No significant differences in yearly or seasonal mean T_{2m} increase, in precipitation or SMB changes were found when using bias-corrected SSC. When using SSC from MIROC-ESM model, the increase in T_{2m} is around +4K in both cases, but the increase in precipitation is +23% when using directly SSC from MIROC-ESM, while it reaches +37% when using corresponding bias-corrected SSC. This difference is found significant and is to be linked with clearly different dynamical and thermodynamical changes in SLP around Antarctica, mainly in winter and spring when using bias-corrected SSC. At the regional scale, large differences in T_{2m} and precipitations increase are found when using bias-corrected SSC both from NorESM1-M and MIROC-ESM.

In this study, we have shown the potential of the ARPEGE model for the study of Antarctic climate and climate change. Un-



surprisingly, the representation of present climate, especially atmospheric general circulation is improved when using observed SSC. When using SSC from NorESM1-M, we found a 10% higher precipitation accumulation at the Antarctic-continent scale with respect to the bias-corrected reference in both historical and future climate. With respect to the observations, NorESM1-M SST are characterized by a weaker meridional gradient in the Southern Ocean, which decreases the strength of Westerlies

5 around Antarctica and favor the meridional transport of moisture towards the Pole.

Concerning climate change signals, we confirm the importance of the choice of the coupled model from which SSC scenario is taken. By performing bias correction of SSC, we showed that not only the regional pattern of temperature and precipitation changes can be different. Indeed, in the case of MIROC-ESM SSC, we found significantly higher precipitation increase and larger increase in winter T_{2m} when using bias-corrected SSC. These results are another argument in favor of the bias correction

10 of SSC when performing future climate scenarios, as it reduces the uncertainty of the baseline (historical) climate and the need for computational resources as only one historical simulation using observed SSC is needed. However, this method still bears some uncertainties for the study of the climate change in Antarctica, mainly coming from the errors of the atmospheric model ARPEGE. We have seen that the errors on atmospheric general circulation remain substantial even when using observed SSC. Therefore, in future work, we will assess the uncertainties associated with the errors of the atmospheric model by perform-

15 ing an ARPEGE simulation nudged towards the reanalysis and use the statistics of the model drift in this nudged simulation such as done in Guldberg et al. (2005) to perform an atmosphere bias-corrected ARPEGE historical simulation. Bias-corrected projections such as in Krinner et al. (2018) can then also be assessed using the methods presented here.



References

- Agosta, C., Favier, V., Krinner, G., Gallée, H., Fettweis, X., and Genthon, C.: High-resolution modelling of the Antarctic surface mass balance, application for the twentieth, twenty first and twenty second centuries, *Climate Dynamics*, 41, 3247–3260, <https://doi.org/10.1007/s00382-013-1903-9>, 2013.
- 5 Agosta, C., Fettweis, X., and Datta, R.: Evaluation of the CMIP5 models in the aim of regional modelling of the Antarctic surface mass balance, *The Cryosphere*, 9, 2311–2321, <https://doi.org/10.5194/tc-9-2311-2015>, 2015.
- Agosta, C., Amory, C., Kittel, C., Orsi, A., Favier, V., Gallée, H., van den Broeke, M. R., Lenaerts, J. T. M., van Wessem, J. M., and Fettweis, X.: Estimation of the Antarctic surface mass balance using MAR (1979–2015) and identification of dominant processes, *The Cryosphere Discussions*, 2018, 1–22, <https://doi.org/10.5194/tc-2018-76>, <https://www.the-cryosphere-discuss.net/tc-2018-76/>, 2018.
- 10 Amory, C., Trouvilliez, A., Gallée, H., Favier, V., Naaim-Bouvet, F., Genthon, C., Agosta, C., Piard, L., and Bellot, H.: Comparison between observed and simulated aeolian snow mass fluxes in Adélie Land, East Antarctica, *The Cryosphere*, 9, 1373–1383, <https://doi.org/10.5194/tc-9-1373-2015>, 2015.
- Arblaster, J. M. and Meehl, G. A.: Contributions of External Forcings to Southern Annular Mode Trends, *Journal of Climate*, 19, 2896–2905, <https://doi.org/10.1175/JCLI3774.1>, 2006.
- 15 Ashfaq, M., Skinner, C. B., and Diffenbaugh, N. S.: Influence of SST biases on future climate change projections, *Climate Dynamics*, 36, 1303–1319, <https://doi.org/10.1007/s00382-010-0875-2>, 2011.
- Beaumont, J., Krinner, G., Déqué, M., Haarsma, R., and Li, L.: Assessing bias-corrections of oceanic surface conditions for atmospheric models, *Geophysical Model Development* (accepted), -, -, <https://doi.org/doi:10.5194/gmd-2017-247>, 2018.
- Boone, A. and Etchevers, P.: An Intercomparison of Three Snow Schemes of Varying Complexity Coupled to the Same Land Surface Model: Local-Scale Evaluation at an Alpine Site, *Journal of Hydrometeorology*, 2, 374–394, [https://doi.org/10.1175/1525-7541\(2001\)002<0374:AIOTSS>2.0.CO;2](https://doi.org/10.1175/1525-7541(2001)002<0374:AIOTSS>2.0.CO;2), 2001.
- Bracegirdle, T. J. and Marshall, G. J.: The Reliability of Antarctic Tropospheric Pressure and Temperature in the Latest Global Reanalyses, *Journal of Climate*, 25, 7138–7146, <https://doi.org/10.1175/JCLI-D-11-00685.1>, 2012.
- Bracegirdle, T. J., Shuckburgh, E., Sallee, J.-B., Wang, Z., Meijers, A. J. S., Bruneau, N., Phillips, T., and Wilcox, L. J.: Assessment of surface winds over the Atlantic, Indian, and Pacific Ocean sectors of the Southern Ocean in CMIP5 models: historical bias, forcing response, and state dependence, *Journal of Geophysical Research: Atmospheres*, 118, 547–562, <https://doi.org/10.1002/jgrd.50153>, 2013.
- 25 Bracegirdle, T. J., Stephenson, D. B., Turner, J., and Phillips, T.: The importance of sea ice area biases in 21st century multimodel projections of Antarctic temperature and precipitation, *Geophysical Research Letters*, 42, 10,832–10,839, <https://doi.org/10.1002/2015GL067055>, 2015.
- 30 Bracegirdle, T. J., Hyder, P., and Holmes, C. R.: CMIP5 Diversity in Southern Westerly Jet Projections Related to Historical Sea Ice Area: Strong Link to Strengthening and Weak Link to Shift, *Journal of Climate*, 31, 195–211, <https://doi.org/10.1175/JCLI-D-17-0320.1>, 2018.
- Bromwich, D. H., Nicolas, J. P., Monaghan, A. J., Lazzara, M. A., Keller, L. M., Weidner, G. A., and Wilson, A. B.: Corrigendum: Central West Antarctica among the most rapidly warming regions on Earth, *Nature Geoscience*, 7, 76, <https://doi.org/http://dx.doi.org/10.1038/ngeo2016>, 2013.
- 35 Clem, K. R., Renwick, J. A., and McGregor, J.: Autumn Cooling of Western East Antarctica Linked to the Tropical Pacific, *Journal of Geophysical Research: Atmospheres*, 123, 89–107, <https://doi.org/10.1002/2017JD027435>, 2018.



- Comiso, J. C. and Nishio, F.: Trends in the sea ice cover using enhanced and compatible AMSR-E, SSM/I, and SMMR data, *Journal of Geophysical Research: Oceans*, 113, <https://doi.org/10.1029/2007JC004257>, <https://agupubs.onlinelibrary.wiley.com/doi/abs/10.1029/2007JC004257>, 2008.
- Delaygue, G., Masson, V., and Jouzel, J.: Climatic stability of the geographic origin of Antarctic precipitation simulated by an atmospheric
5 general circulation model, *Annals of glaciology*, 29, 45–48, 1999.
- Déqué, M., Dreveton, C., Braun, A., and Cariolle, D.: The ARPEGE/IFS atmosphere model: a contribution to the French community climate
modelling, *Climate Dynamics*, 10, 249–266, <https://doi.org/10.1007/BF00208992>, 1994.
- Favier, V., Krinner, G., Amory, C., Gallée, H., Beaumet, J., and Agosta, C.: Antarctica-Regional Climate and Surface Mass Budget, *Current
Climate Change Reports*, 3, 303–315, <https://doi.org/10.1007/s40641-017-0072-z>, 2017.
- 10 Fettweis, X., Gallée, H., Lefebvre, F., and van Ypersele, J.-P.: Greenland surface mass balance simulated by a regional climate model and
comparison with satellite-derived data in 1990–1991, *Climate Dynamics*, 24, 623–640, <https://doi.org/10.1007/s00382-005-0010-y>, <https://doi.org/10.1007/s00382-005-0010-y>, 2005.
- Fréville, H., Brun, E., Picard, G., Tatarinova, N., Arnaud, L., Lanconelli, C., Reijmer, C., and van den Broeke, M.: Using MODIS land
surface temperatures and the Crocus snow model to understand the warm bias of ERA-Interim reanalyses at the surface in Antarctica, *The
15 Cryosphere*, 8, 1361–1373, <https://doi.org/10.5194/tc-8-1361-2014>, <https://www.the-cryosphere.net/8/1361/2014/>, 2014.
- Frieler, K., Clark, P. U., He, F., Buizert, C., Reese, R., Ligtenberg, S. R. M., van den Broeke, M., Winkelmann, R., and Levermann, A.:
Consistent evidence of increasing Antarctic accumulation with warming, *Nature Climate Change*, 5, <https://doi.org/10.1038/nclimate2574>,
<http://dx.doi.org/10.1038/nclimate2574>, 2015.
- Gallée, H. and Schayes, G.: Development of a Three-Dimensional Meso-Y Primitive Equation Model: Katabatic Winds Sim-
20 ulation in the Area of Terra Nova Bay, Antarctica, *Monthly Weather Review*, 122, 671–685, [https://doi.org/10.1175/1520-0493\(1994\)122<0671:DOATDM>2.0.CO;2](https://doi.org/10.1175/1520-0493(1994)122<0671:DOATDM>2.0.CO;2), 1994.
- Gallée, H., Preunkert, S., Argentini, S., Frey, M. M., Genthon, C., Jourdain, B., Pietroni, I., Casasanta, G., Barral, H., Vignon, E., Amory, C.,
and Legrand, M.: Characterization of the boundary layer at Dome C (East Antarctica) during the OPALÉ summer campaign, *Atmospheric
Chemistry and Physics*, 15, 6225–6236, <https://doi.org/10.5194/acp-15-6225-2015>, <https://www.atmos-chem-phys.net/15/6225/2015/>,
25 2015.
- Genthon, C., Krinner, G., and Castebrunet, H.: Antarctic precipitation and climate-change predictions: horizontal resolution and margin vs
plateau issues, *Annals of Glaciology*, 50, 55–60, <https://doi.org/10.3189/172756409787769681>, 2009.
- Giorgi, F. and Gutowski, W. J.: Coordinated Experiments for Projections of Regional Climate Change, *Current Climate Change Reports*, 2,
202–210, <https://doi.org/10.1007/s40641-016-0046-6>, 2016.
- 30 Guldberg, A., Kaas, E., Déqué, M., Yang, S., and Vester, T.: Reduction of systematic errors by empirical model correction: impact on
seasonal prediction skill, *Tellus A*, 57, 575–588, <https://doi.org/10.1111/j.1600-0870.2005.00120.x>, 2005.
- Hernández-Díaz, L., Laprise, R., Nikiéma, O., and Winger, K.: 3-Step dynamical downscaling with empirical correction of sea-surface
conditions: application to a CORDEX Africa simulation, *Climate Dynamics*, 48, 2215–2233, <https://doi.org/10.1007/s00382-016-3201-9>,
2017.
- 35 Jones, P. D. and Harpham, C.: Estimation of the absolute surface air temperature of the Earth, *Journal of Geophysical Research: Atmospheres*,
118, 3213–3217, <https://doi.org/10.1002/jgrd.50359>, <https://agupubs.onlinelibrary.wiley.com/doi/abs/10.1002/jgrd.50359>, 2013.
- Krinner, G. and Flanner, M. G.: Striking stationarity of large-scale climate model bias patterns under strong climate change, *Proc. Natl. Acad.
Sci.*, in press., -, -, <https://doi.org/->, 2017.



- Krinner, G., Genthon, C., Li, Z.-X., and Le Van, P.: Studies of the Antarctic climate with a stretched-grid general circulation model, *Journal of Geophysical Research: Atmospheres*, 102, 13 731–13 745, <https://doi.org/10.1029/96JD03356>, <http://dx.doi.org/10.1029/96JD03356>, 1997.
- Krinner, G., Guicherd, B., Ox, K., Genthon, C., and Magand, O.: Influence of Oceanic Boundary Conditions in Simulations of Antarctic Climate and Surface Mass Balance Change during the Coming Century, *Journal of Climate*, 21, 938–962, <https://doi.org/10.1175/2007JCLI1690.1>, 2008.
- Krinner, G., Rinke, A., Dethloff, K., and Gorodetskaya, I. V.: Impact of prescribed Arctic sea ice thickness in simulations of the present and future climate, *Climate Dynamics*, 35, 619–633, <https://doi.org/10.1007/s00382-009-0587-7>, 2010.
- Krinner, G., Langeron, C., Ménégoz, M., Agosta, C., and Brutel-Vuilmet, C.: Oceanic Forcing of Antarctic Climate Change: A Study Using a Stretched-Grid Atmospheric General Circulation Model, *Journal of Climate*, 27, 5786–5800, <https://doi.org/10.1175/JCLI-D-13-00367.1>, 2014.
- Krinner, G., Beaumet, J., Favier, V., Déqué, M., and Brutel-Vuilmet, C.: Regional climate projections with empirical run-time bias correction, *Journal of Advances in Modeling Earth Systems*, (submitted), 2018.
- Kushner, P. J., Held, I. M., and Delworth, T. L.: Southern Hemisphere Atmospheric Circulation Response to Global Warming, *Journal of Climate*, 14, 2238–2249, [https://doi.org/10.1175/1520-0442\(2001\)014<0001:SHACRT>2.0.CO;2](https://doi.org/10.1175/1520-0442(2001)014<0001:SHACRT>2.0.CO;2), 2001.
- Lefebvre, F., Fettweis, X., Gallée, H., Van Ypersele, J.-P., Marbaix, P., Greuell, W., and Calanca, P.: Evaluation of a high-resolution regional climate simulation over Greenland, *Climate Dynamics*, 25, 99–116, <https://doi.org/10.1007/s00382-005-0005-8>, 2005.
- Lenaerts, J. T. M., Vizcaino, M., Fyke, J., van Kampenhout, L., and van den Broeke, M. R.: Present-day and future Antarctic ice sheet climate and surface mass balance in the Community Earth System Model, *Climate Dynamics*, 47, 1367–1381, <https://doi.org/10.1007/s00382-015-2907-4>, 2016.
- Ligtenberg, S. R. M., van de Berg, W. J., van den Broeke, M. R., Rae, J. G. L., and van Meijgaard, E.: Future surface mass balance of the Antarctic ice sheet and its influence on sea level change, simulated by a regional atmospheric climate model, *Climate Dynamics*, 41, 867–884, <https://doi.org/10.1007/s00382-013-1749-1>, 2013.
- Massonnet, F., Fichet, T., Goosse, H., Bitz, C. M., Philippon-Berthier, G., Holland, M. M., and Barriat, P.-Y.: Constraining projections of summer Arctic sea ice, *The Cryosphere*, 6, 1383–1394, 2012.
- Moss, R. H., Edmonds, J. A., Hibbard, K. A., Manning, M. R., Rose, S. K., Van Vuuren, D. P., Carter, T. R., Emori, S., Kainuma, M., Kram, T., et al.: The next generation of scenarios for climate change research and assessment, *Nature*, 463, 747, 2010.
- Nicolas, J. P. and Bromwich, D. H.: New Reconstruction of Antarctic Near-Surface Temperatures: Multidecadal Trends and Reliability of Global Reanalyses, *Journal of Climate*, 27, 8070–8093, <https://doi.org/10.1175/JCLI-D-13-00733.1>, 2014.
- Noilhan, J. and Mahfouf, J.-F.: The ISBA land surface parameterisation scheme, *Global and Planetary Change*, 13, 145 – 159, [https://doi.org/https://doi.org/10.1016/0921-8181\(95\)00043-7](https://doi.org/https://doi.org/10.1016/0921-8181(95)00043-7), <http://www.sciencedirect.com/science/article/pii/0921818195000437>, soil Moisture Simulation, 1996.
- Orr, A., Marshall, G. J., Hunt, J. C. R., Sommeria, J., Wang, C.-G., van Lipzig, N. P. M., Cresswell, D., and King, J. C.: Characteristics of Summer Airflow over the Antarctic Peninsula in Response to Recent Strengthening of Westerly Circumpolar Winds, *Journal of the Atmospheric Sciences*, 65, 1396–1413, <https://doi.org/10.1175/2007JAS2498.1>, 2008.
- Palermo, C., Genthon, C., Claud, C., Kay, J. E., Wood, N. B., and L'Ecuyer, T.: Evaluation of current and projected Antarctic precipitation in CMIP5 models, *Climate Dynamics*, 48, 225–239, <https://doi.org/10.1007/s00382-016-3071-1>, <https://doi.org/10.1007/s00382-016-3071-1>, 2017.



- Pollard, D., DeConto, R. M., and Alley, R. B.: Potential Antarctic Ice Sheet retreat driven by hydrofracturing and ice cliff failure, *Earth and Planetary Science Letters*, 412, 112 – 121, <https://doi.org/https://doi.org/10.1016/j.epsl.2014.12.035>, 2015.
- Previdi, M. and Polvani, L. M.: Anthropogenic impact on Antarctic surface mass balance, currently masked by natural variability, to emerge by mid-century, *Environmental Research Letters*, 11, 094 001, <http://stacks.iop.org/1748-9326/11/i=9/a=094001>, 2016.
- 5 Ritz, C., Tamsin, E. L., Durand, G., Payne, A. J., Peyaud, V., and Hindmarsh, R. C. A.: Potential sea-level rise from Antarctic ice-sheet instability constrained by observations, *Nature*, 528, 115, <https://doi.org/http://dx.doi.org/10.1038/nature16147>, 2015.
- Salas y Méliá, D.: A global coupled sea ice-ocean model, *Ocean Modelling*, 4, 137 – 172, [https://doi.org/https://doi.org/10.1016/S1463-5003\(01\)00015-4](https://doi.org/https://doi.org/10.1016/S1463-5003(01)00015-4), <http://www.sciencedirect.com/science/article/pii/S1463500301000154>, 2002.
- Stroeve, J. C., Kattsov, V., Barrett, A., Serreze, M., Pavlova, T., Holland, M., and Meier, W. N.: Trends in Arctic sea ice extent from CMIP5, 10 CMIP3 and observations, *Geophysical Research Letters*, 39, n/a–n/a, <https://doi.org/10.1029/2012GL052676>, 2012.
- Taylor, K., Williamson, D., and Zwiers, F.: The sea surface temperature and sea-ice concentration boundary condition for AMIP II simulations, PCMDI Rep. 60, Program for Climate Model Diagnosis and Intercomparison, Lawrence Livermore National Laboratory, Livermore, CA, 25 pp., 2000.
- Taylor, K. E., Stouffer, R. J., and Meehl, G. A.: An overview of CMIP5 and the experiment design, *Bulletin of the American Meteorological Society*, 93, 485–498, 2012.
- 15 Turner, J., Colwell, S. R., Marshall, G. J., Lachlan-Cope, T. A., Carleton, A. M., Jones, P. D., Lagun, V., Reid, P. A., and Iagovkina, S.: The SCAR READER Project: Toward a High-Quality Database of Mean Antarctic Meteorological Observations, *Journal of Climate*, 17, 2890–2898, [https://doi.org/10.1175/1520-0442\(2004\)017<2890:TSRPTA>2.0.CO;2](https://doi.org/10.1175/1520-0442(2004)017<2890:TSRPTA>2.0.CO;2), [https://doi.org/10.1175/1520-0442\(2004\)017<2890:TSRPTA>2.0.CO;2](https://doi.org/10.1175/1520-0442(2004)017<2890:TSRPTA>2.0.CO;2), 2004.
- 20 Turner, J., Bracegirdle, T. J., Phillips, T., Marshall, G. J., and Hosking, J. S.: An Initial Assessment of Antarctic Sea Ice Extent in the CMIP5 Models, *Journal of Climate*, 26, 1473–1484, <https://doi.org/10.1175/JCLI-D-12-00068.1>, 2013.
- Turner, J., Hosking, J. S., Bracegirdle, T. J., Marshall, G. J., and Phillips, T.: Recent changes in Antarctic Sea Ice, *Philosophical Transactions of the Royal Society of London A: Mathematical, Physical and Engineering Sciences*, 373, <https://doi.org/10.1098/rsta.2014.0163>, <http://rsta.royalsocietypublishing.org/content/373/2045/20140163>, 2015.
- 25 Turner, J., Lu, H., White, I., King, J. C., Phillips, T., Hosking, J. S., Bracegirdle, T. J., Marshall, G. J., Mulvaney, R., and Deb, P.: Absence of 21st century warming on Antarctic Peninsula consistent with natural variability, *Nature*, 535, –, <https://doi.org/10.1038/nature18645>, 2016.
- Turner, J., Phillips, T., Marshall, G. J., Hosking, J. S., Pope, J. O., Bracegirdle, T. J., and Deb, P.: Unprecedented springtime retreat of Antarctic sea ice in 2016, *Geophysical Research Letters*, 44, 6868–6875, <https://doi.org/10.1002/2017GL073656>, <https://agupubs.onlinelibrary.wiley.com/doi/abs/10.1002/2017GL073656>, 2017.
- 30 van Lipzig, N. P. M., King, J. C., Lachlan-Cope, T. A., and van den Broeke, M. R.: Precipitation, sublimation, and snow drift in the Antarctic Peninsula region from a regional atmospheric model, *Journal of Geophysical Research: Atmospheres*, 109, <https://doi.org/10.1029/2004JD004701>, 2004.
- Vaughan, D. G., Bamber, J. L., Giovinetto, M., Russell, J., and Cooper, A. P. R.: Reassessment of Net Surface Mass Balance in Antarctica, *Journal of Climate*, 12, 933–946, [https://doi.org/10.1175/1520-0442\(1999\)012<0933:RONSMB>2.0.CO;2](https://doi.org/10.1175/1520-0442(1999)012<0933:RONSMB>2.0.CO;2), 1999.
- 35 Vaughan, D. G., Marshall, G. J., Connolley, W. M., Parkinson, C., Mulvaney, R., Hodgson, D. A., King, J. C., Pudsey, C. J., and Turner, J.: Recent Rapid Regional Climate Warming on the Antarctic Peninsula, *Climatic Change*, 60, 243–274, 2003.



Competing interests. The authors have no competing interests.

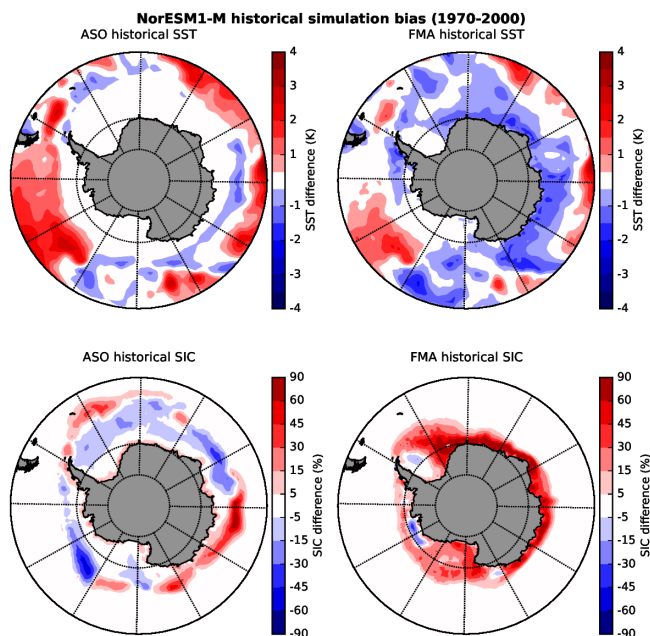
Acknowledgements. This study was funded by the Agence Nationale de la Recherche through contract ANR-14-CE01-0001-01 (ASUMA) and ANR-15-CE01-0003 (APRES3). We acknowledge the World Climate Research Programme's Working Group on Coupled Modelling, which is responsible for CMIP, and we thank the climate modeling groups participating to CMIP5 for producing and making available their
5 model output. For CMIP the U.S. Department of Energy's Program for Climate Model Diagnosis and Intercomparison provides coordinating support and led development of software infrastructure in partnership with the Global Organization for Earth System Science Portals. The Centre National de Recherches M'et'eorologique (M'et'e-France, CNRS) and associated colleagues are warm-fully thanks for providing resources and help to run ARPEGE model.
We also thank the Scientific Committee on Antarctic Research, SCAR and the British Antarctic Survey for the availability of the MET
10 READER data base.

Appendix A: Sea Surface Conditions

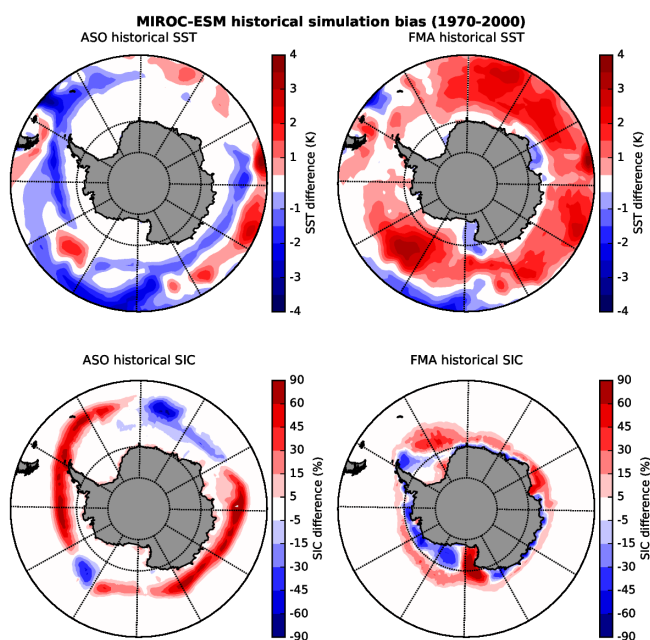
In this section, the historical bias in SSC in MIROC-ESM and NorESM1-M (Fig. A1) used to force ARPEGE model as well as the differences between SSC in rcp8.5 scenarios in these model and their bias-correction (Fig. A2). These first two figures illustrate the efficiency of the bias-correction methods fro SSC as the similarity between differences in futures SST is striking.
15 For SIC, the patterns of the model bias in historical climates can easily be identified in the differences between original and bias-corrected SSC (Fig. A2), but because there is a decrease of SIE, these patterns are shifted poleward. Yearly and seasonal Southern hemisphere SIE in MIROC-ESM, NorESM1-M and observations (Table A1) and in the two AOGCM original and bias-corrected rcp8.5 scenario (Table A2) are also presented in this supplementary material. Here again, the efficiency of the bias-correction methods to reproduce the climate change signal in hemispheric SIE from the coupled model can be confirmed.
20 In Figure A3, SST historical bias for both coupled model for each seasons on the whole Southern hemisphere are displayed in order to support the discussion on how the atmospheric model has responded to the same SST biases or perturbations in present and future climate. Table A2, the climate change signals in SIE in scenarios from MIROC-ESM and NorESM1-M can be evaluated, with the decrease in sea-ice being three time more important in MIROC-ESM scenarios. It can also be noted that both AOGCM hemispheric SIE are quite close to the observations. Only an underestimate of about 20% of Summer and Fall
25 SIE in MIROC-ESM can be mentioned. As a consequence, there are few differences in both absolute and relative changes as well as in absolute values in bias-corrected and original projected SIE.

Appendix B: Near-surface temperature

In this section, we present additional material for near-surface temperatures (T_{2m}). A map showing the location different research stations including those of the MET reader data base used for the comparison with ARPEGE presented in Tab. 3 can
30 be seen in Fig. B1.

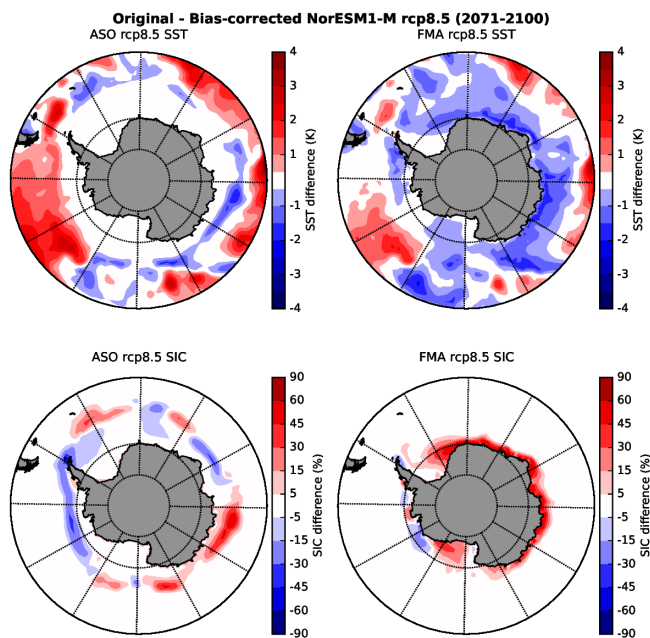


(a) NorESM1-M historical

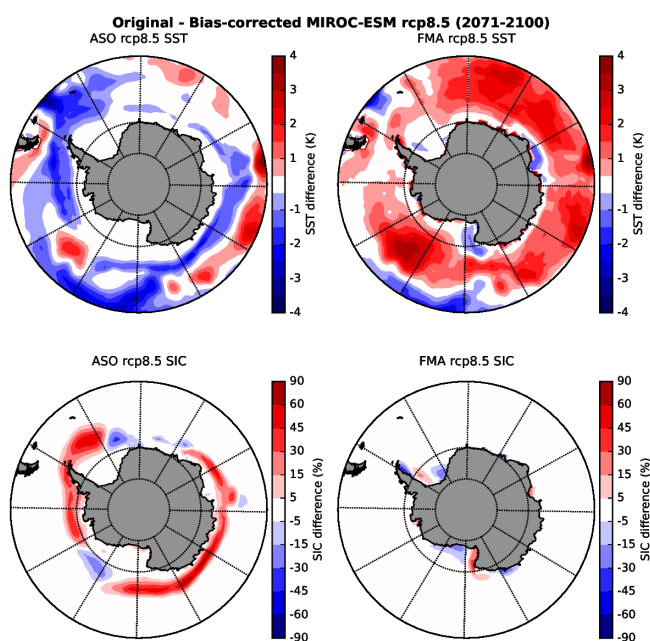


(b) MIROC-ESM historical

Figure A1. Bias in SST (*top*) and SIC (*bottom*) for late winter, August, September, October (*left*) and summer, February, March, April (*right*) historical simulations of (a) NorESM1-M and (b) MIROC-ESM.

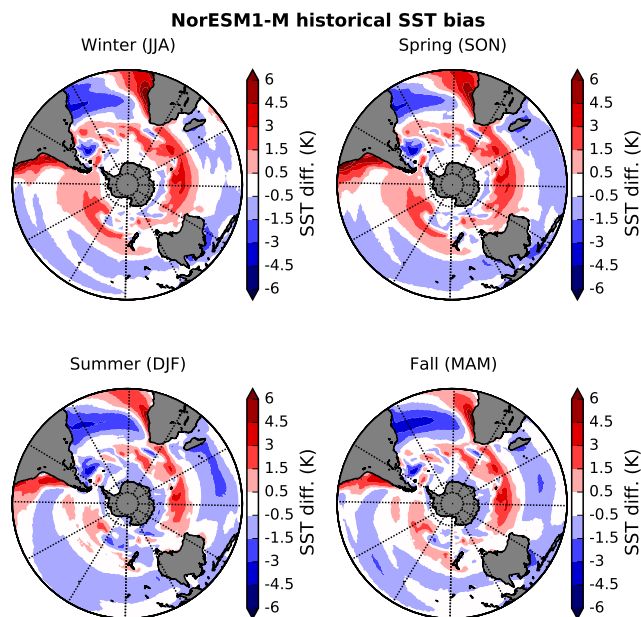


(a) NorESM1-M RCP8.5

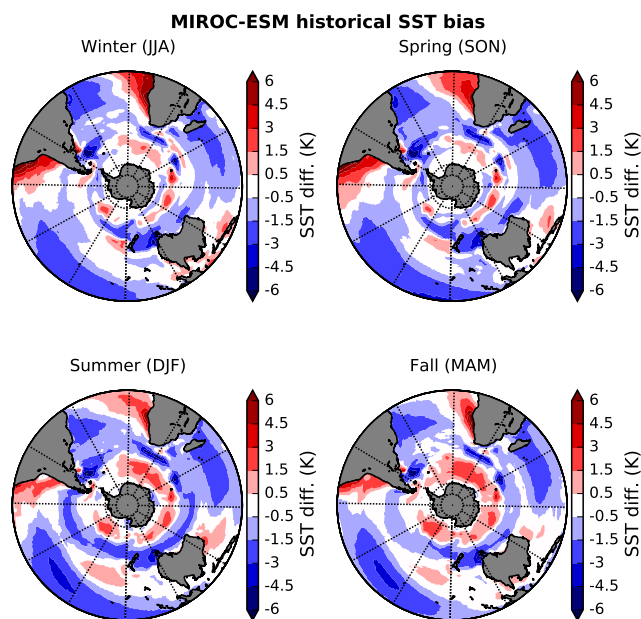


(b) MIROC-ESM RCP8.5

Figure A2. Same as Fig.A1 but for RCP8.5 scenario and corresponding bias corrected SSC



(a) NorESM1-M historical



(b) MIROC-ESM historical

Figure A3. Seasonal historical bias in SST in the Southern hemisphere from NorESM1-M (*top*) and MIROC-ESM (*bottom*).



Table A1. Annual and seasonal Southern Hemisphere mean historical Sea Ice Extent (SIE, 10^6 km^2) in observations, NorESM1-M and MIROC-ESM.

	Year	DJF	MAM	JJA	SON
Observations	9.6	4.4	5.6	13.5	14.7
NorESM1-M	9.8	4.8	6.6	14.0	15.4
MIROC-ESM	8.9	3.1	4.0	13.3	15.3

Table A2. Annual and seasonal Southern Hemisphere mean projected Sea Ice Extent and absolute change with respect to historical climate (10^6 km^2) in NorESM1-M and MIROC-ESM rcp8.5 scenarios and corresponding bias-corrected SSC.

	Year	DJF	MAM	JJA	SON
NorESM1-M-rcp85	8.2	4.0	5.1	11.7	13.6
<i>Change (10^6 km^2)</i>	<i>-1.6</i>	<i>-0.8</i>	<i>-1.5</i>	<i>-2.3</i>	<i>-1.8</i>
NorESM1-M-rcp85-bc	7.9	3.5	4.2	11.1	12.7
<i>Change (10^6 km^2)</i>	<i>-1.6</i>	<i>-0.8</i>	<i>-1.5</i>	<i>-2.3</i>	<i>-1.8</i>
MIROC-ESM-rcp85	4.2	0.9	1.2	6.8	8.2
<i>Change (10^6 km^2)</i>	<i>-4.7</i>	<i>-2.2</i>	<i>-2.8</i>	<i>-6.5</i>	<i>-7.2</i>
MIROC-ESM-rcp85-bc	4.2	1.0	1.5	6.8	7.6
<i>Change (10^6 km^2)</i>	<i>-5.3</i>	<i>-3.4</i>	<i>-4.1</i>	<i>-6.7</i>	<i>-7.1</i>

The effect of introducing biased SSC on the modelling of Antarctic T_{2m} with ARPEGE AGCM is also presented in Fig. B2. For ARP-NOR-20 (Fig. B2a), the introduction of biased SSC increase the warm bias on the East Antarctic Plateau with respect to MAR and weather stations already present in ARP-AMIP (Fig. 4). The same statement can be made for the winter cold bias over the Peninsula. In summer, there are relatively few differences in the skills of the latter two simulation, which is consistent with similar errors on large-scale atmospheric circulation (Fig. 2).

For ARP-MIR-20 (Fig. B2a), the cold bias over the Peninsula is also larger than ARP-AMIP in both seasons. The winter warm bias over the EAP is similar than in ARP-AMIP. In summer, the general tendency of ARP-MIR-20 to be cooler than ARP-AMIP over the continent leads to a decrease of the warm bias with respect to MAR over the margins of the EAIS and WAIS on one hand, but increase the cold bias on the EAP on the other hand, which can be seen in the differences with MAR and weather stations.

Appendix C: Precipitation

In this section, the effects of driving ARPEGE with biased SSC (NorESM1-M an MIROC-ESM) on the modelling of Antarctic precipitation are presented trough comparisons with MAR-ERA-I total precipitation. Differences between ARP-AMIP, ARP-NOR-20 and ARP-MIR-20 with MAR-ERA-I for total precipitations are show in Fig. C1. Mean error and RMSE with respect

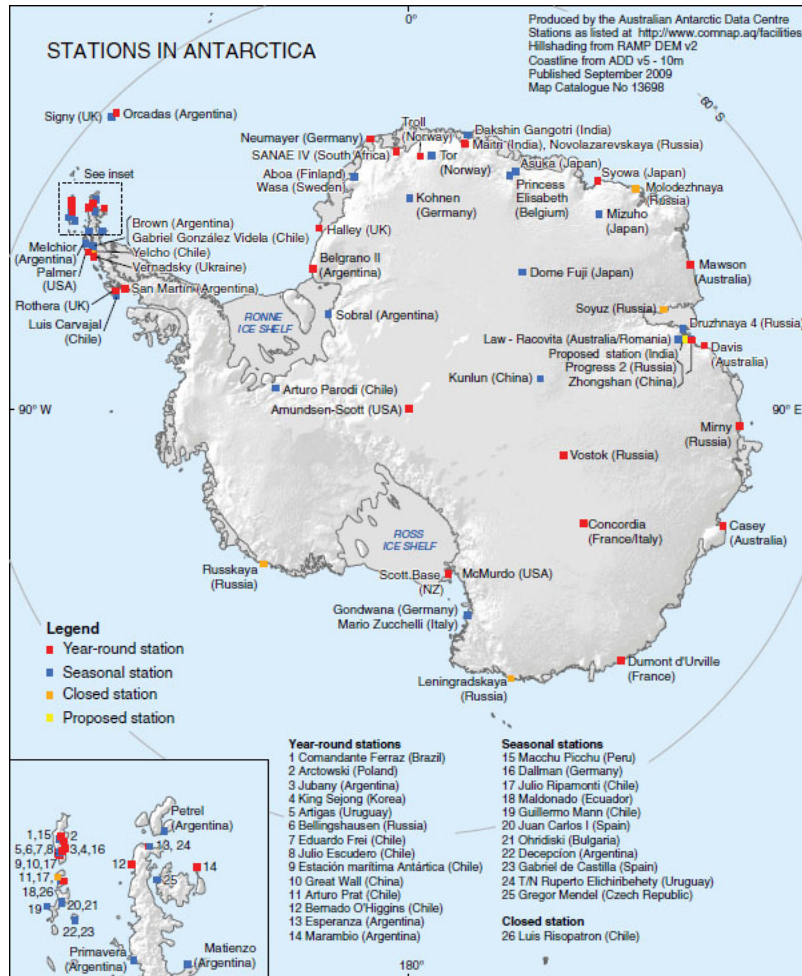
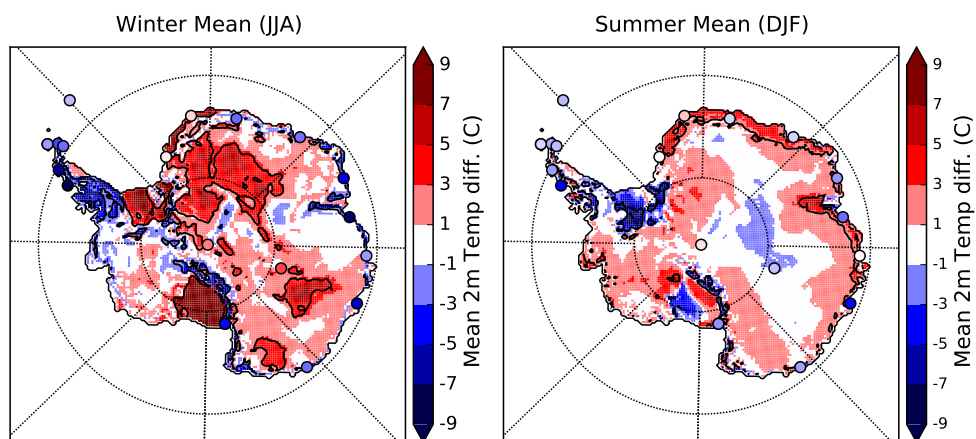


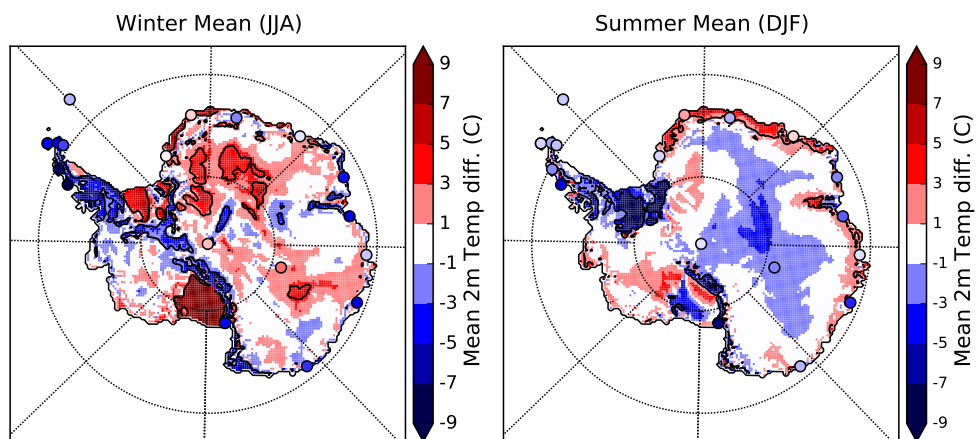
Figure B1. Map showing the location of Antarctic research stations including those from the MET READER data base. **Credit : Australian Antarctic Data Centre**

to MAR are presented in the upper-left corner. The pattern of the errors is quite similar for each simulation. Unsurprisingly, the best agreement (smaller RMSE) with MAR is found the ARP-AMIP simulation. The wet biases with respect to MAR over Dronning Maud and Marie-Byrd Land already present in ARP-AMIP tend to increase in both ARP-NOR-20 and ARP-MIR-20 simulations. The ARP-NOR-20 simulation has systematic wet bias (larger mean error) with respect to MAR at the continent

5 scale consistent with the 10% increase in precipitation integrated over the whole ice sheet found in this simulation with respect to ARP-AMIP.



(a) ARP-NOR-20



(b) ARP-MIR-20

Figure B2. T_{2m} differences between ARP-NOR-20 (*top*) and ARP-MIR-20 (*bottom*) and MAR-ERA-I simulations in winter (JJA, *left*) and summer (DJF, *right*) for the reference period 1981-2010. Circles are T_{2m} differences between ARP-AMIP and weather stations from the READER data base. Black contour lines represent areas where $|ARPEGE - MAR| > 1.1MAR\sigma$.

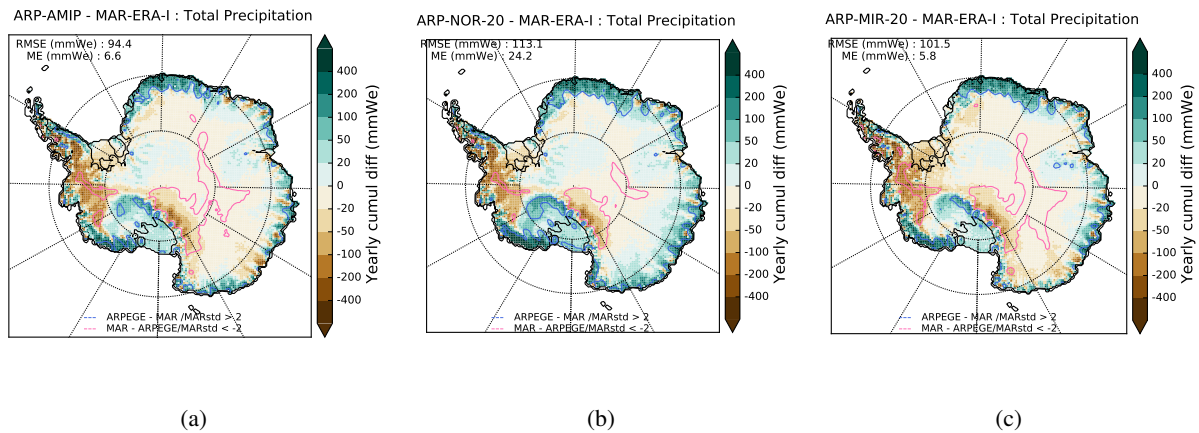


Figure C1. ARP-AMIP(*top*), ARP-NOR-20(*centre*) and ARP-MIR-20(*bottom*) minus MAR-ERA-I total precipitation. Pink and blue contour lines indicates where difference is larger than two MAR standard deviation ($2\text{-}\sigma$). RMSE and mean error with respect to MAR are indicated in the upper-left corner.

Appendix D: Atmospheric general circulation

D1 Present climate

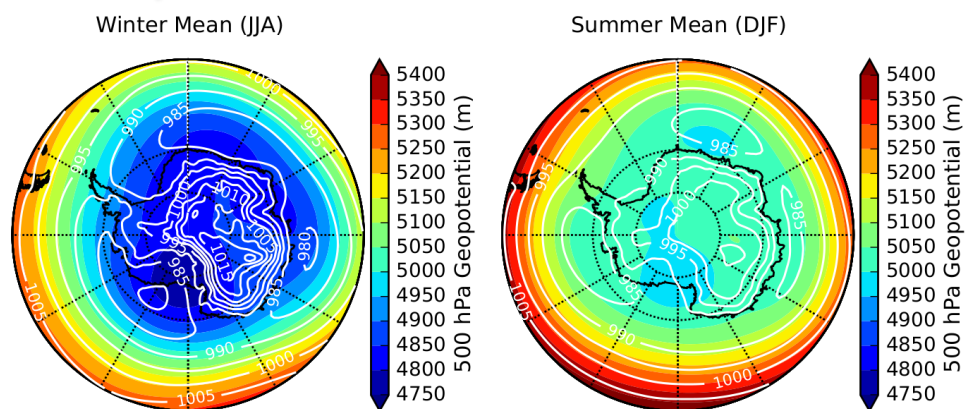
In this section, we present and discuss the ability of ARPEGE atmospheric model to represent the broad features of the atmospheric general circulation around Antarctica. The winter (JJA) and summer (DJF) 500 hPa geopotentials and sea-level pressures (SLP) for ERA-I reanalyses and the ARP-AMIP simulation are presented in Fig. D1. In winter, it can be seen that ARPEGE reproduces quite correctly the 3 climatological minimum in SLP and the localization of the maximum of the South Polar vortex above the Ross Sea rather than on the South Pole. However, as already mentioned, the depth of the three SLP minimum and the meridional gradient around 50 to 60°S is underestimated. This remark is also valid in summer. It can also be noted that ARPEGE reproduces relatively correctly the displacement of the third SLP minima (Amundsen Sea Low) from eastern Ross Sea in winter to the Bellingshausen Sea, west of the Peninsula in summer.

D2 Consistency of the atmospheric model response

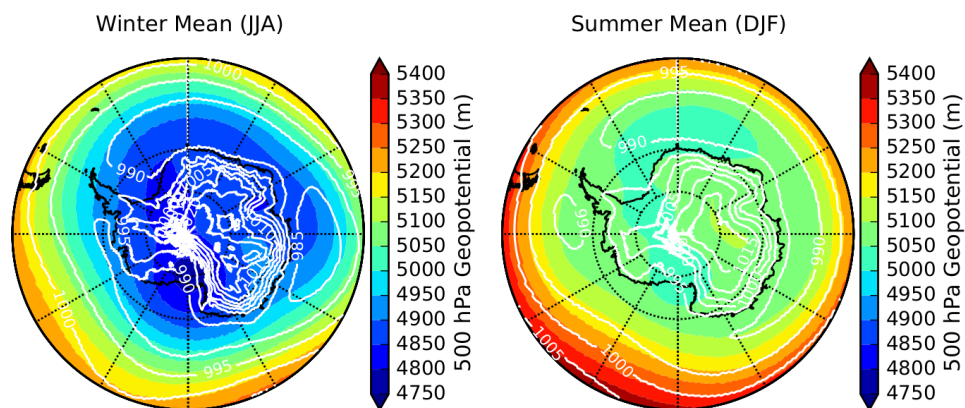
In this section, we briefly discuss the consistency of the response of the atmospheric model ARPEGE when forced by similar SSC between present and future climate mentioned in the discussion. For the similarity of the SSC bias, see Fig. A1 and Fig. A2. This consistency of the atmospheric model response is considered as being the key for having similar climate signals between climate projections realized with or without bias corrected SSC. In Fig. D2, the difference in SLP between ARP-NOR-20 and ARP-AMIP for the four climatological seasons is shown on the upper part, and the corresponding difference for future climate (ARP-NOR-21-ARP-NOR-21-OC) is shown on the lower part. It can be seen that there are few changes in the differences pattern between present and future climate which is to be related with the minor differences in climate changes



5 signal found for many variables in the experiment with bias-corrected and original NorESM1-M SSC. In Fig. D3, the same differences for the experiment performed with MIROC-ESM SSC are displayed. Here again, the pattern of the differences are very similar. We note however a tripole in the difference for future climate (ARP-MIR-21 - ARP-MIR-21-OC) in autumn (MAM), which was absent in the difference for present climate. This tripole can certainly be related to the tripole observed for the differences in precipitation and sea-level pressure change signal observed in Section 3.2.

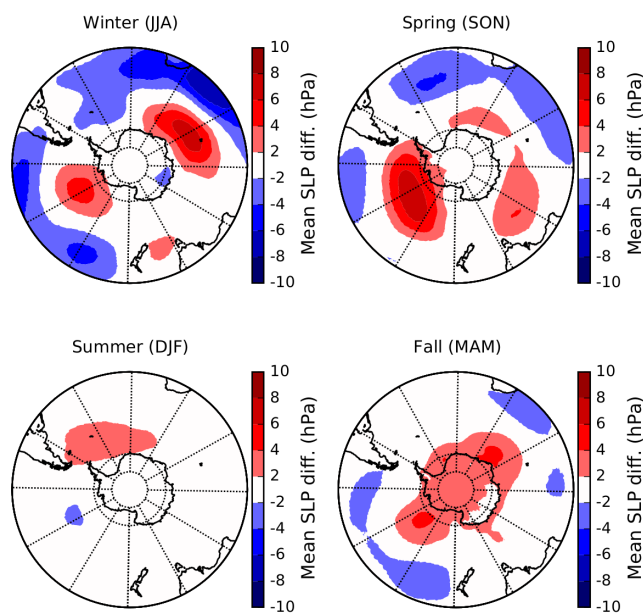


(a) ERA-Interim

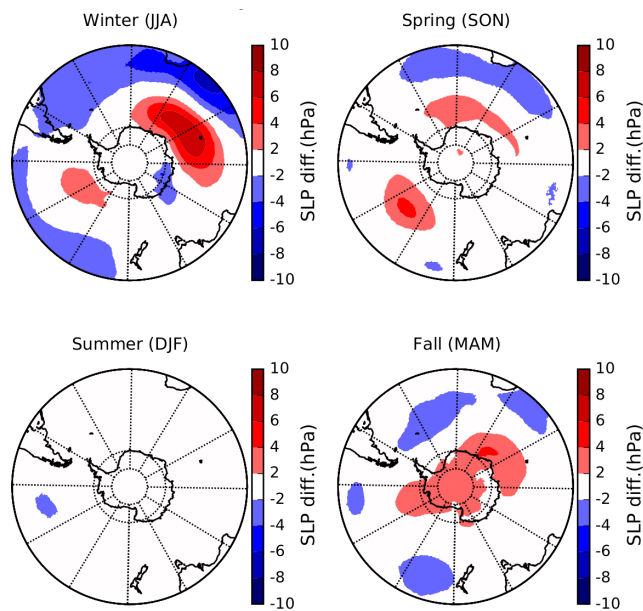


(b) ARP-AMIP

Figure D1. ERA-Interim (*top*) and ARP-AMIP(*right*) 500 hPa geopotentials (shadings) and sea-level pressures (white contour lines) in winter (*left*) and summer (*right*) for the reference period 1981-2010.

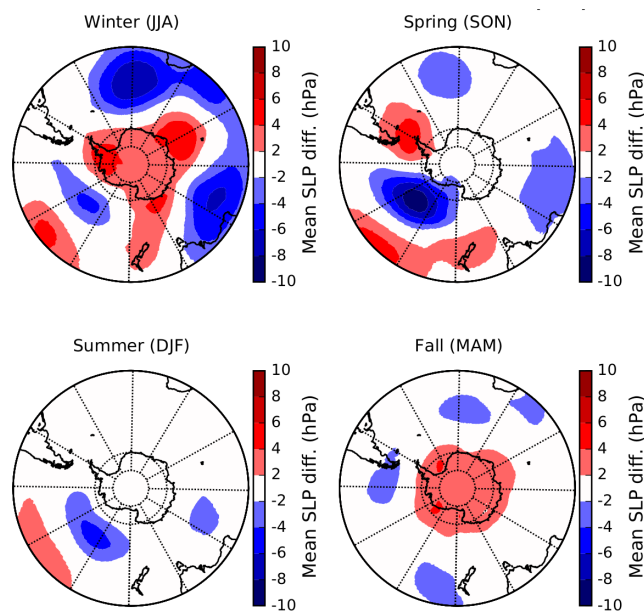


(a) ARP-NOR-20 - ARP-AMIP

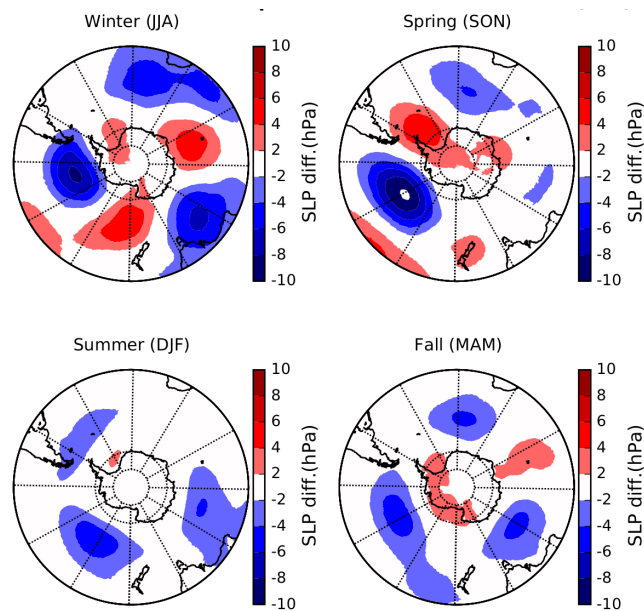


(b) ARP-NOR-21 - ARP-NOR-21-OC

Figure D2. Difference between ARP-NOR-20 and ARP-AMIP for seasonal sea-level pressure (*top*) and corresponding differences for late 21st century, ARP-NOR-21 minus ARP-NOR-21-OC



(a) ARP-MIR-20 - ARP-AMIP



(b) ARP-MIR-21 - ARP-MIR-21-OC

Figure D3. Difference between ARP-MIR-20 and ARP-AMIP for seasonal sea-level pressure (*top*) and corresponding differences for late 21st century, ARP-MIR-21 minus ARP-MIR-21-OC